JAEA-Technology
2007-064

# Design Study of the Optical System in the Port Plug for Edge Thomson Scattering Diagnostics for ITER

Shin KAJITA, Takaki HATAE, Atsushi KATSUNUMA* and Yoshinori KUSAMA

ITER Diagnostics Group
Fusion Research and Development Directorate

January 2008

Japan Atomic Energy Agency

日本原子力研究開発機構

本レポートは日本原子力研究開発機構が不定期に発行する成果報告書です。
本レポートの入手並びに著作権利用に関するお問い合わせは、下記あてにお問い合わせ下さい。
なお、本レポートの全文は日本原子力研究開発機構ホームページ（http://www.jaea.go.jp/index.shtml）より発信されています。このほか財団法人原子力弘済会資料センター*では実費による複写頒布を行っております。

〒319-1195　茨城県那珂郡東海村白方白根 2 番地 4
日本原子力研究開発機構　研究技術情報部　研究技術情報課
電話 029-282-6387, Fax 029-282-5920

*〒319-1195　茨城県那珂郡東海村白方白根 2 番地 4　日本原子力研究開発機構内

This report is issued irregularly by Japan Atomic Energy Agency
Inquiries about availability and/or copyright of this report should be addressed to
Intellectual Resources Section, Intellectual Resources Department,
Japan Atomic Energy Agency
2-4 Shirakata Shirane, Tokai-mura, Naka-gun, Ibaraki-ken 319-1195 Japan
Tel +81-29-282-6387,　Fax +81-29-282-5920

# Design Study of the Optical System in the Port Plug for Edge Thomson Scattering Diagnostics for ITER

Shin KAJITA※, Takaki HATAE, Atsushi KATSUNUMA* and Yoshinori KUSAMA

Division of ITER Project
Fusion Research and Development Directorate
Japan Atomic Energy Agency, Naka-shi, Ibaraki-ken

(Received November 7, 2007)

The design of the collection optics for edge Thomson scattering diagnostics for ITER is provided. Since the neutron and gamma ray radiation fluxes generated by the nuclear fusion reaction are considerably high near the plasma in ITER, available optical components are limited. Near the plasma, namely in the front-end optics, only metal mirrors can be used; moreover, optical fiber may be used only outside the vacuum window, which is located far from the front-end optics. In this design, three metal mirrors are used for the front-end optics, and the light ray is transmitted in the slender port plug through a relay optical system. To compensate the aberrations and increase the coupling efficiency to the fibers, two types of optical system with Catadioptric system are proposed for fiber-coupling optical system. It has been revealed that refraction type and reflection type system are not adequate for the fiber-coupling optical system. The image qualities are discussed based on the ray tracing analysis for the Catadioptric optical system.

Keywords: ITER, Thomson Scattering, Optical Design, Relay Optics, Catadioptric System, Optical Fiber

---

※Senior Post-Doctoral Fellow
*Nikon Corporation

# ITER 周辺トムソン散乱計測用光学系の設計研究

日本原子力研究開発機構　核融合研究開発部門
ITER プロジェクトユニット
梶田　信※，波多江　仰紀，勝沼　淳*，草間　義紀

(2007 年 11 月 7 日　受理)

ITER 周辺トムソン散乱計測用光学系の設計研究を行った。設計に際しては、核融合反応により発生する中性子やγ線など、放射線によって使用可能な光学部品が制限される。プラズマ近傍の先端部光学系では金属ミラーのみ使用可能であり、光学ファイバーは先端部光学系から距離を離して設置される真空窓の外でのみ使用可能となる。本設計研究においては、先端部光学系に三枚の金属ミラーを用い、その後リレー光学系でポート外部へとイメージを伝送する構成とした。ファイバー結合光学系において反射方式や屈折方式では十分な性能を得ることができないことが明らかになった。色収差を補正し、かつファイバーの結合特性を向上させるために、反射方式と屈折方式の利点を合せたカタディオプトリック方式を用いた二つの光学系を設計し、両者のスペックと性能の比較を行った。スポットダイアグラムなどの結果から、カタディオプトリック方式の光学系における結像性能を議論する。

那珂核融合研究所（駐在）：〒311-0193　茨城県那珂市向山 801-1
※任期付研究員
*ニコン（株）

Contents

目次

## 1. Introduction

Laser Thomson scattering is a powerful method to measure the local electron temperature $T_e$ and density $n_e$ simultaneously in high temperature plasmas. Four types of Thomson scattering measurement systems are considered to be installed in ITER[1]. One of the systems is used for the measurement of the edge plasma ($\rho$>0.9, where $\rho$ is the normalized minor radius). The required $T_e$ and $n_e$ ranges for the measurement are, 50 eV – 10 keV, and $5\times10^{18}$ - $3\times10^{20}$ $m^{-3}$, respectively, with an accuracy of less than 10%. To satisfy these requirements, it is necessary to provide high-energy laser pulses and a high performance detection system including collection optical system. With regard to the laser system, the laser oscillator with single-longitudinal mode has been developed based on the design study[2], and the high power amplifier for the laser is now developing by use of phase conjugate mirror based on stimulated Brillouin scattering (SBS)[3], which has been successfully used for the high-power laser in the Thomson scattering system for JT-60U[4]. The pulse energy of 5 J and the repetition frequency of 100 Hz is a goal of the laser development. In this report, the discussion mainly focuses on the collection optics for the edge Thomson scattering measurement in ITER, and the optical system for laser transmission.

Table 1-1 shows the key parameters for the collection optics. The optical systems in the port plug for the edge Thomson scattering in ITER can be separated into two systems, i.e. the optical system for laser transmission and that for collecting the scattered photons. The former consists of several mirrors to transmit the laser to the plasma edge region. The latter includes a several mirrors, a relay optical system, a vacuum window, a fiber coupling optical system, and optical fiber bundles.

Since burning plasmas are produced in ITER, there is concern that optical components are easily damaged by the exposure to the neutron and gamma ray fluxes. For the first mirror, the damage due to the charge-exchange neutral atoms should be considered in addition. In particular, the transmittance of lenses or fibers may be significantly degraded by neutrons and gamma rays if they are used without the arrangement to shield the radiation. For mirrors, it is said that dielectric multi-layer mirror may not be used in the port plug because of the influence of the radiation; therefore, metals are candidates of the mirror material in the front-end optics in the port plug.

In the previous design[1,5], the vacuum window and the fiber bundle were penetrated into the port plug. However, it has been estimated from the neutron analysis that the effect of the neutron and gamma ray radiation to the vacuum window and the fibers cannot be neglected in the design[6]. Figure 1-1 shows the evaluation of the neutron flux for the optics. The neutron fluence for vacuum-window was estimated to be $1.4\times10^{17}$ n/cm$^2$, which is the marginal dose to use silica glass. Moreover, the fluence for the fiber was estimated to be $7\times10^{17}$ n/cm$^2$. Optical fibers are considered to be very vulnerable to heavy irradiation in general; the irradiation can lead to some transmission loss[7]. Therefore, it was necessary to redesign the collection optics by considering the radiation effect.

In the present report, the design study of the collection optics is provided based on the previous design by reconsidering the radiation effects. In particular, the concepts of the relay optical system and the fiber-coupling optical system are modified. Moreover, until now, only the conceptual design of the collection optical system has been reported; the detailed design including the locations of the optical components are exhibited in the present study. The overview of the optical systems is presented in Sec. 2. The detailed arrangement of the fiber coupling optical system is shown in Sec. 3. In Sec 4, the characteristics and performance of the optical system is presented. Conclusions and future works are provided in Sec 5.

## 2. Overview of the optical system

### 2.1 Optical system for laser transmission

The optical system for laser transmission consists of several mirrors. The laser beam is focused at the measurement point by use of an off-axis parabolic mirror. The chromatic aberration is not produced because refractors are not used. The optical window for the vacuum boundary should not be normal to the laser axis. If the Brewster viewing port cannot be used from the limitation of the space, the window should be slightly tilted not to reflect back the laser beam to the laser system. After injecting the laser beam through the optical window, laser beam is transmitted to the off-axis parabolic mirror by using a plane mirror, as shown in Fig. 2-1. These two mirrors make up a dogleg structure; the structure reduces the neutron and gamma ray fluxes toward the outside. The reduction of the radiation flux is important not only from the safety point of view, but also from the aspect of the damages in the optics and window materials caused by the exposure to the fluxes. The focal point of the off-axis parabolic mirror is the center of the measurement region. The major specifications of the optical systems are summarized in table 2-1.

### 2.2 Collection Optical system

The collection optical system collects the scattered photons and plasma light; moreover, it transmits images of the laser beam to the optical fiber bundle. Since the optical fiber can be damaged by the exposure to the neutron and gamma ray radiation, it is better to locate it outside the vacuum chamber. However, it also requires a long slender case, in which scattered light ray is transmitted. It is necessary to satisfy the following two conditions for realizing this configuration:

Requirement I: Forming images at least once until the front face of the optical fiber

Requirement II: Forming real images of a pupil in the optical system.

Pupil is the image of an aperture stop, which is an aperture diaphragm to determine the diameter of the light ray that transmits the optical system. The pupil image that can be seen from the light entrance side is termed *entrance pupil*, whereas the pupil image that can be seen from the light exit side is termed *exit pupil*. The intermediate image and image of the pupil are formed one after the other as real images not as virtual images. It makes possible to eliminate the divergence of the light ray caused during the process of the image relay, and consequently, we can form a slender optical system. This is a general method when arranging optics; and a periscope is a typical example by using this method.

By considering the shape of the port plug chassis, it appears to be reasonable to form the first intermediate image in the middle of the chassis, second image around the vacuum window port, and the image of pupil between the second and first intermediate images. The optical system is arranged with the following principles:

- The radiation flux is high in the front-end part of the chassis, which is close to the plasma.

There is concern that transmittance of optical material drastically decreases by the exposure to the radiation. Because the reflectivity of mirrors is less affected by the exposure to the radiation, only mirrors are used for the optical components in the front-end part of the chassis.

- Moreover, a coating or coated components such as anti-reflective (AR) coating and the dielectric multi-layer mirror were not used. It is because they may be easily damaged by the exposure to the radiation.
- Only three mirrors were used in the port plug in order not to deteriorate in the transmissivity of the optical system.
- Only highly purified quartz were used for the lens material in the port plug.
- Fiber coupling optical system is located outside the vacuum chamber to be accessed easily.

Figure 2-2 shows the schematic diagram of the collection optical system consists of front-end optics, relay optics, and fiber coupling optics. In the following sections, the detail arrangements of the optical systems are presented.

### 2.2.1 Mirrors and radiation-shielding slit

Only mirrors are used in the front-end optics. This is because refractors such as lens are easily damaged by the exposure to the radiation. Three mirrors are located in the eccentric configuration, which forms the first intermediate image. At present, the candidate of the first mirror is a rhodium plane mirror because the rhodium has rather high reflectivity in a wide wavelength range of 400 – 1100 nm. Silver has better reflectivity than the rhodium; however, silver is vulnerable to neutron and gamma ray irradiation[8)] Moreover, from the perspective of the sputtering due to the charge-exchange neutral atoms, rhodium is a plausible choice because of its low sputtering rate[9)]. As for the second and third mirrors, aluminum is a candidate material because of its high reflectivity in the wavelength range. Second mirror is a convex toroidal mirror and the third mirror is a concave cylindrical mirror. Ray aberration can be reduced by use of toroidal and cylindrical mirrors. Since the ray hits the mirrors at an angle, astigmatism occurs when using a normal concave spherical mirror. The toroidal and cylindrical surfaces are generally used for reducing astigmatism, so that they are used in the present arrangement. Coating technique does not applied to the mirrors in the chassis because there is concern that the coating is easily damaged by the exposure to the radiation. Experimental investigations are necessary for the durability of the courting to the high-dose radiation. In the present study, it is assumed that polished material is used for reflection surface.

A slit is placed at the image point that is formed with the mirrors as shown in Fig. 2-2. This slit transmits only the light rays and works on reducing radiation.

### 2.2.2 Relay optics

Relay optics is located between the slit and vacuum window. It forms the second intermediate

image, which is a conjugate image of the first intermediate image, just outside the vacuum window. Since refractors can be easily damaged by the exposure to the radiation, it is plausible that only mirrors are used for the optics in the chassis. However, the reflectivity of metal mirror without coating is not so high; moreover, a mirror optics requires much space than the optics with lenses. Therefore, the relay optics consists only of mirrors is unrealistic. Since the slit reduces the neutron and gamma fluences, it is considered that the lenses can be used in the relay optics.

Highly purified quartz is used for lenses without anti-reflective coating. The relay optical system consists of a field lens and a relay lens. The field lens is a single double-convex lens, and the relay lens is a single plane-convex lens. The function of the field lens is to form the image of the second mirror, which corresponds to the aperture stop. In the precise manner, the first pupil is formed right after the relay lens. The function of the relay lens is to form the second image, which is the conjugate image of the first image, right after the vacuum window. These two components are located coaxially. The shape of the field lens becomes slender because only the central narrow part is used.

Since only quartz refractors are used in the relay optical system, large chromatic aberration is generated. The front-end optical system does not produce chromatic aberration, since only mirrors are used. However, in other words, it cannot compensate the chromatic aberration produced by the other optics. Therefore, the fiber coupling optics, which is located after the relay optics, must have the function to compensate the chromatic aberration, which is produced with the relay optics. Without the fiber coupling optics, the chromatic aberration causes strong wavelength dependence on the coupling efficiency to the fiber bundle.

A plain quartz plate without anti-reflective coating is used for the vacuum window. The plate should be slightly tilted against the window not to reflect back the laser beam to the laser system.

### 2.2.3 Fiber coupling optics and optical fiber bundle

A fiber coupling optics is located outside the vacuum vessel port to form the last image, which is a conjugate image of the second intermediate image. Because the influence of the radiation outside the vacuum vessel port is not so significant, it is not necessary to consider the effects. Two types of the optical arrangement, Type-I and II, are proposed in Sec. 3.

Optical fibers are arranged to fit the final images that are formed by the fiber coupling optics. The design of the optical fiber has not been decided yet; it is assumed to use the quartz multi-mode optical fibers. In the ray tracing analysis presented in Sec. 4, a fiber with the core diameter of 0.2 mm, and the numerical aperture of 0.2 is used. Both Type-I and II were arranged not to exceed the numerical aperture of 0.2. An optical fiber bundle with multiple fibers will be used to collect the ray from a measurement point. The fiber end is cut at perpendicular with respect to the axis of the fiber optic cable. It is important to arrange the fiber bundles by aligning the angle of each bundle so that

all of them see the center of the exit pupil.

## 3. Detailed arrangements of the fiber coupling optical system

In Sec. 2.2.3, the fiber coupling optics was presented in brief. It is required for this optical system to compensate the chromatic aberrations produced in the relay optical system and itself, namely, in the fiber coupling optics. In this section, we discuss the optimum optical system by comparing the characteristics of several arrangements with different design schemes.

### 3.1 Refraction type system

Refraction type refers here to an optical system consists of only refractors, i.e. lenses. The durability of radiation is not so important for the fiber coupling optical system because its location is rather far from the plasma surface in addition to the slit for neutron shielding. Therefore, an achromatic design by use of low dispersion lenses is one of the candidates. Although the wavelength range for the measurement is very wide, approximately 400 – 1100 nm, it may be possible from the technical point of view to compensate the chromatic aberration if low dispersion lenses can be used. However, in a practical sense, it is impossible to arrange it.

For reference, the schematic of the optical arrangement for the refraction type system is shown in Fig. 3-1. Because of the size limitation of the optical glass in the production process, many lenses are necessary to compensate the chromatic aberration. The design in Fig. 3-1 has not been completed.

The achromatic design uses multiple positive and negative power lenses. In order to compensate the chromatic aberration produced in the relay optical system, the transmittance at short wavelength becomes significantly low because the volume of the lenses is very large. Therefore, we do not discuss the refraction type system further in this report.

### 3.2 Reflection type system

Reflection type system refers here to an optical system consists of only mirrors. Reflection type system has an advantage that it does not produce chromatic aberration. However, conversely, it also cannot compensate the chromatic aberration that is produced in the relay optical system. Moreover, the reflection type system produces other aberrations such as astigmatism, and consequently, abnormally large system is necessary to compensate them. Therefore, in a practical sense, it is impossible to arrange the optical system utilizing only mirrors.

### 3.3 Catadioptric system

A catadioptric system produces little chromatic aberration. Furthermore, it can compensate aberrations including chromatic one in a reasonable volume. In the catadioptric system, mirrors have power for imaging, and lenses have a function to compensate Seidel's five aberrations, i.e., spherical aberration, coma aberration, astigmatism, curvature of image field, and distortion. The catadioptric system produces little aberrations generally; moreover, the imaging performance can be better than

the optical system utilizing only mirrors. Schmidt camera, and Maksutov camera are the typical catadioptric system.

We assumed to use quartz for the lens material because of its high transmittance. We do not use aspheric surfaces; only spherical surfaces are used. It is expected to use coating technique to avoid the corrosion of the surface, which degraded the surface reflectivity. However, several problems are remained with regard to the coating for the lens. Although it is plausible to use a multi-layer coating, which makes possible to reduce the reflectivity lower than 1% in a wide wavelength range, the coating layer may be damaged due to the surface stress when it is cooled in the production process because the diameter of the lens is considerably large. Size of large lens becomes >400 mm in diameter. Since the layer number increases as expanding the wavelength range, it may be necessary to reconsider the wavelength range for the collection optics. With regard to the mirrors, concave mirrors with silver surface are used.

The locations of the optical elements in Type-I and Type-II are shown in table A-1, and A-2, respectively (Appendix A) in the coordination with respect to the center position of the inner plane of the vacuum window port. In addition, in appendix A, the lens data in CODE-V[10] format in Type-I and II are presented.

### 3.3.1 Arrangement of catadioptric system (Type-I)

The arrangement Type-I consists of field lens, correction lens, and mirror-lens. Figure 3-2(a), (b) and (c) show the three-dimensional diagrams of the Type-I arrangement from different eye views. The field lens is located coaxially with the relay optics. On the other hand, the field lens, correction lens, and mirror-lens are located in a relatively eccentric manner to reduce the image blur caused by the chromatic aberration. The field lens forms the second pupil, which is a image of the first pupil, near the mirror-lens. The ray goes through the field lens one-way, whereas it goes and returns between the correction lens and mirror-lens. The final image, which is a conjugate image of the second intermediate image, is formed by the correction lens and mirror-lens.

A plane mirror is located between the correction lens and the fiber bundle to change the direction of the ray not to interfere with the fiber bundle. A silver mirror with a protective overcoat can be used for the plane mirror. Because the curvature of image field is not corrected, the last image is distorted to have a convex shape on the side of the mirror.

One disadvantage in Type-I is in chromatic aberration of magnification. The chromatic aberration of magnification is the difference in the magnification of the image caused by the difference in the wavelength. The details are discussed in Sec. 4.

### 3.3.2 Arrangement of catadioptric system (Type-II)

The arrangement Type-II is similar to that of Type-I. Figure 3-3(a), (b) and (c) show the

three-dimensional diagrams of Type-II arrangement from different eye views. The characteristics of Type- II are as follows:

- Two lenses are used for the relay lens optics in Type-II, whereas only one lens is used in Type-I
- The fiber coupling optical system in Type-II is longer than that of Type-I,
- The last image is distorted, having a concave shape on the mirror side.

A longer fiber coupling optical system results in the reduction of the chromatic aberration of magnification. It is suggested that the increase in the length between the pupil and the mirror-lens improves the chromatic aberration of magnification. However, the size of the mirror-lens becomes may be larger than the available space because the position of the mirror-lens is significantly shifted from that of the pupil.

# 4. Characteristics of the optical system

## 4.1 Coordination and angle definition

Here, the definition of the coordination and angle used in the following ray tracing analysis by use of CODE-V[10] are presented. Figure 4-1 shows the coordinates and definition of the angles used for the analysis. Principally, the *z*-axis corresponds to the light axis or normal direction to the optical element. Ray goes on to the positive direction. The *x*-axis and *y*-axis correspond to the longitudinal and transversal directions, respectively. Figure 4-2 shows the schematic diagram representing typical five measurement points used for the analysis and the relation to the entrance pupil. In table 4-1, important parameters used for the analysis at the five measurement points are presented. The distance $y_{laser}$ represents the direction along the laser beam with the zero point at F3.

## 4.2 Image point and ray direction

In the present optical system, the ray direction is not normal to the image surface; the image surface tilts with respect to the plane that is normal to the ray direction. Furthermore, the image surface is not a plane but curves. Therefore, it is necessary to align the position and angle of the fibers by considering the image point and the ray direction.

Tables 4-2 and 4-3 show the image point and direction of the chief ray for Type-I and Type-II, respectively. The chief ray is the ray that passes through the center of the aperture stop. Based on the position shown in Table 4-2 or Table 4-3, the fiber position should be aligned; moreover, to increase the coupling efficiency, the fiber angle should be at least fitted to the angle $\alpha$. It is noted that the displacement also exists in *x*-direction.

## 4.3 Projection magnification

The projection magnifications in longitudinal and transversal directions are different in the present optical system. The projection magnifications in transversal and longitudinal directions are shown in Tables 4-4 (Type-I) and 4-5 (Type-II). Here, *x* and *y* directions correspond to the radial and axial directions of the laser beam, respectively. The definitions are different from those defined in Sec. 4.1. The image surface was assumed to be the face surface of the optical fiber. The sign indicate the direction of the image.

## 4.4 Spot diagram of the optical system

Figure 4-3 and 4-4 show the analysis results of the optical image quality by means of spot diagram for Type-I and Type-II arrangements, respectively. In those figures, (a) shows the case, in which light ray emits from the laser beam position to the optical fiber, whereas (b) shows the case, in which light ray emits from the position of the optical fiber to the laser beam. Five measurement positions (F1-F5) are used for the analysis. The wavelengths used for the analysis are 1100, 1000, 900, 800,

700, 600, 500 and 400 nm.

In Type-I, the position of the spots changes as changing the wavelength particularly at the edge region of the measurement position. It is noted that the eye view is slightly shifted toward the laser beam transmission direction in some wavelength range. It can be said that Type-II has a better optical image quality than that of Type-I in terms of the chromatic aberration. In terms of the spatial resolution, we can see from Figs. 4-3, and 4-4 that the blur, namely the resolution normal to beam, is less than 1 cm, which is the requirement shown in Table 1.1, in both Type-I and Type-II. On the other hand, the resolution along the laser beam does not satisfy the requirement of 1.5 cm in Type-I, at the edge region in particular.

### 4.5 Image of the optical fiber

In addition to the spot diagram, we present the simulation results of the illumination profile emitted from a fiber. The scope of the fiber can be understood from the simulation. We used the same measurement points and wavelengths as the spot diagram shown in Sec. 4.4.

Figure 4-5, 4-6, 4-7, 4-8, and 4-9 show the images and contour plots of the illumination profile from the fiber for the measurement points F1, F2, F3, F4, and F5, respectively. The optics arrangement is Type-I. In the same manner, the images and contour plots of the illumination profile for the Type-II arrangement are shown in Fig. 4-10, 4-11, 4-12, 4-13, and 4-14.

In both Type-I and II, we can see that the blur, namely the resolution normal to beam, is smaller than 1 cm. On the other hand, the image size along the laser beam in Type-I is rather long, particularly in F1. From the contour plot of Type-I, the image length along the laser beam is 2 cm in F1, which is longer than the required resolution of 1.5 cm. In Type-II, on the other hand, it seems that the image size is comparable or slightly smaller than the required resolution of 1 cm in vertical direction to the laser beam and 1.5 cm along the laser beam.

### 4.6 Image shift due to the displacement of optical elements

The light path may be displaced when the vacuum chamber is distorted. Since the conjugate relation must be satisfied between the image of the laser beam and the optical fiber, it is necessary to compensate the displacement of the light path when the displacement amount is not neglected. Here, we discuss the effect of the displacement of each optical components based on the table of the optical eccentric displacement shown in appendix B. The displacement of the light path is calculated in cases that each optical components are shifted in $x$, $y$, and $z$ directions or tilt around $x$, $y$, and $z$ directions. The shift amount and the tilt angle were assumed to be +1 mm, and +0.1 degree, respectively. In the calculation, the effect of the vacuum window was neglected, and the fiber coupling optics was assumed to be a rigid system, which resulted in no relative displacements of components.

The tables give us the information of the light ray shift due to the distortion of the vacuum chamber. We can understand how to compensate the shift by aligning the optical components. It seems thus far that the alignment of the fiber bundle is sufficient to compensate the image shift. If the alignment of the fiber bundle is not sufficient to compensate the image shift, fiber-coupling optics should be moved entirely with fixing the optics inside the vacuum chamber. Since the large number of the table is necessary to present all the data, the image shift due to the displacements of the field lens 1 are shown in appendix B.

In the tables, the shifts for an optical component, the name of which is shown in the leftmost field, are presented in the same row. The row without the name corresponds to the value on the imaginary plane. The image shift for the measurement points F1, F3, and F5 are presented. The coordination of the optical components is the specific one, but *x*-, and *y*-directions correspond to roughly vertical, and horizontal directions, respectively.

## 5. Conclusion and future work

The design of the collection optics for the edge Thomson scattering diagnostics for ITER is provided, and the optical components that can be used in the optics are discussed. The optical system for collection optics consists of mainly three parts, mirrors and radiation-shielding slit, relay optics, and fiber coupling optics. Two types of optical systems using the Catadioptric system in the fiber coupling optics are proposed. Type-I has a compact size fiber coupling optics, while the Type-II has a rather large lens in the fiber coupling optics. Based on the analysis with spot diagram and so on, it has been evaluated that the performance of Type-II is superior to that of Type-I.

With regard to the resolution, it can be said that it is necessary to use Type-II to satisfy the requirement. However, larger space is necessary when Type-II is used, and the space may be larger than the available space; it is necessary to check the available space for the fiber coupling optics.

Concerning the lenses in the fiber coupling optical system, it is necessary to check whether anti-reflective multi-layer coating can be used. Moreover, with regard to a mirror-lens in the fiber coupling optical system, it is necessary to check whether dielectric multi-layer mirror can be used.

The material choice for the laser transmission has not been investigated in this study. It is necessary to consider the degradation of the reflectivity due to the exposure to the neutral particle and radiation (neutron and gamma ray). Thus far, only metal mirror has been considered, it is attractive if multi-layer coating mirror can be used for in-vessel laser transmission mirrors because the reflectivity is greater than 99 %. In Ref. 11), multi-layer coating mirror has been exposed to neutron flux, but the reduction of the reflectivity was not observed. Only few studies have been reported related with the effect of the radiation on the multi-layer coating mirror; further experimental investigation is necessary to confirm the durability of the multi-layer coating mirrors.

References

1) Design Description Document (DDD) ITER diagnostic system, (WBS5.5) July, 2000.

2) T. Hatae, H. Kubomura, S. Matsuoka, and Y. Kusama : “Desing of Single-Longitudinal-mode Laser Oscillator for Edge Thomson Scattering System in ITER”, JAEA-Technology (2006) 2006-021.

3) T. Hatae, O. Naito, S. Kitamura, T. Sakuma, and T. Hamano : “Applications of Stimulated Brillouin Scattering Phase Conjugate Mirror to Thomson Scattering Diagnostics in JT-60U and ITER”, J. Korean Phys. Soc. 49 S160(2006).

4) H. Yoshida, M. Nakatsuka, T. Hatae, S. Kitamura, T. Sakuma, and T. Hamano : “Two-Beam-Combined 7.4 J, 50 Hz Q-switch Pulsed YAG Laser System Based on SBS Phase Conjugation Mirror for Plasma Diagnostics”, Jpn. J. Appl. Phys. 43 L1038 (2004).

5) P. Nielsen, “Proceedings of 10$^{th}$ International Symposium on Laser-Aided Plasma Diagnostics”, 401 (2001).

6) N. Kusama: private communication.

7) T. Shikama, T. Kakuta, M. Narui, T. Sagawa, N. Shamoto, T. Uramoto, K. Sanada, and H. Kayano : “Behavior of radiation-resistant optical fibers under irradiation in a fission reactor”, J. Nucl. Mater. 212-215 421 (1994).

8) Y. Murakami, *et al.* “Radiation databook” (in Japanese), Chijinshokan, Tokyo, pp.121-124 (1982).

9) V. S. Voitsenya, V. G. Konovalov, M. F. Becker, O. Motojima, K. Narihara, and B. Schunke: “Materials selection for the in situ mirrors of laser diagnostics in fusion devices”, Rev. Sci. Instrum. 70 2016 (1999).

10) CODE-V (Optical design & analysis software) (online)
available from http://www.opticalres.com/cv/cvprodds_f.html (accessed 2007-10-22).

11) I.I.Orlovskiy, K.Yu.Vukolov: “Thermal and neutron tests of multilayered dielectric mirrors”, Fusion Engineering Design 74 865 (2005).

Table 1-1 Key parameters for the collection optics

| Parameter | Value | comment |
|---|---|---|
| wavelength range | 400-1100 nm | |
| *f* number | < 10 | |
| Resolution | < 1.5 cm | Along beam |
| Blur | < 1 cm | Normal to beam |

Table 2-1: Major specifications of the optical systems for laser transmission.

| | |
|---|---|
| Distance between the off-axis mirror and its focal point | 5197.5 mm |
| Laser beam diameter | 100 mm |
| Focal F number | F/52 |
| Length of the measurement region | 675 mm |
| Maximum laser beam diameter in the measurement region | 6.5 mm |
| Laser wavelength | 1064 nm<br>(for diagnostics) |
| Focal length of the parabolic mirror | 1396.05 mm |
| Distance from the paraboloid axis to the reflection axis (off-axis quantity) | 4607.67 mm |

Table 4-1: Important parameters used for the analysis at typical five measurement points. The distance $y_{laser}$ represents the direction along the laser beam with the zero point at F3, $L$ is the distance from the entrance pupil, $\theta$ is the angle between the chief ray and vertical directions, and $\omega$ is the ray angle from the F3 ray.

| Measurement points | $y_{laser}$ [mm] | $L$ [mm] | $\theta$ [degree] | $\omega$ [degree] | Solid angle |
|---|---|---|---|---|---|
| F1 | 389.0 | 2198.79 | -64.4024 | 5.1966 | 0.0064713 |
| F2 | 194.5 | 2025.13 | -62.0242 | 2.8184 | 0.0076510 |
| F3 | 0.0 | 1855.60 | -59.2058 | 0.0000 | 0.0091239 |
| F4 | -143.0 | 1734.31 | -56.7865 | -2.4193 | 0.0104354 |
| F5 | -286.0 | 1616.57 | -54.0092 | -5.1966 | 0.0119722 |

Table 4-2: Image points and the direction of the chief ray for Type-I optical arrangement at five measurement positions (F1-F5).

| measurement position | | image point and the direction of the chief ray | | | | |
|---|---|---|---|---|---|---|
| | $y_{laser}$ [mm] | $x$ [mm] | $y$ [mm] | $z$ [mm] | $\alpha$ [°] | $\beta$ [°] |
| F1 | 389 | -3.260 | 65.653 | -33.469 | 1.50272 | -0.19194 |
| F2 | 194.5 | -2.661 | 36.827 | -18.225 | 1.17725 | -0.53971 |
| F3 | 0 | -2.020 | 2.353 | -0.448 | 0.06495 | -0.81927 |
| F4 | -143 | -1.489 | -28.008 | 18.076 | -0.93885 | -0.97050 |
| F5 | -286 | -0.778 | -63.488 | 41.314 | -1.44669 | -1.05069 |

Table 4-3: Image points and the direction of the chief ray for Type-II optical arrangement at five measurement positions (F1-F5).

| measurement position | | image point and the direction of chief ray | | | | |
|---|---|---|---|---|---|---|
| | $y_{laser}$ [mm] | $x$ [mm] | $y$ [mm] | $z$ [mm] | $\alpha$ [°] | $\beta$ [°] |
| F1 | 389 | -2.550 | 62.460 | -31.828 | 3.85627 | -0.23548 |
| F2 | 194.5 | -2.036 | 37.723 | -18.483 | 2.55111 | -0.52367 |
| F3 | 0 | -1.477 | 8.198 | -4.038 | 0.11332 | -0.78605 |
| F4 | -143 | -1.006 | -17.312 | 8.000 | -2.03460 | -0.96821 |
| F5 | -286 | -0.482 | -46.704 | 22.500 | -3.69831 | -1.14748 |

Table 4-4 Projection magnifications in transversal ($m_x$) and longitudinal ($m_y$) directions in the case of the projection from laser beam to fiber, and its inverse in the case of the projection from fiber to laser beam. (Type-I)

| measurement point | From laser to fiber | | Fiber to laser beam | |
|---|---|---|---|---|
| | $m_x$ | $m_y$ | $1/m_x$ | $1/m_y$ |
| F1 | -0.329 | 0.139 | -3.040 | 7.180 |
| F2 | -0.358 | 0.162 | -2.796 | 6.158 |
| F3 | -0.394 | 0.196 | -2.535 | 5.107 |
| F4 | -0.427 | 0.227 | -2.342 | 4.398 |
| F5 | -0.462 | 0.261 | -2.166 | 3.836 |

Table 4-5 Projection magnifications in transversal ($m_x$) and longitudinal ($m_y$) directions in the case of the projection from laser beam to fiber, and its inverse in the case of the projection from fiber to laser beam. (Type-II)

| measurement point | From laser to fiber | | Fiber to laser beam | |
|---|---|---|---|---|
| | $m_x$ | $m_y$ | | $m_x$ |
| F1 | -0.271 | 0.115 | -3.684 | 8.721 |
| F2 | -0.299 | 0.135 | -3.346 | 7.403 |
| F3 | -0.334 | 0.165 | -2.994 | 6.056 |
| F4 | -0.365 | 0.193 | -2.742 | 5.179 |
| F5 | -0.398 | 0.222 | -2.510 | 4.496 |

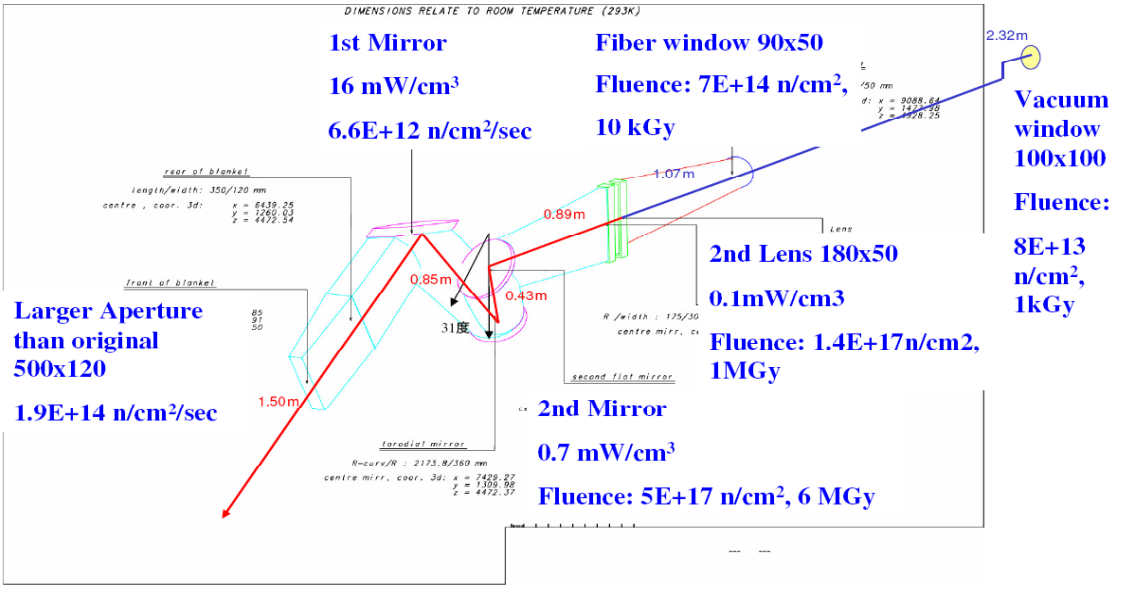


Fig 1.1 Estimation results of the neutron flux and gamma ray absorbed dose for the optics in the previous optical design[6].

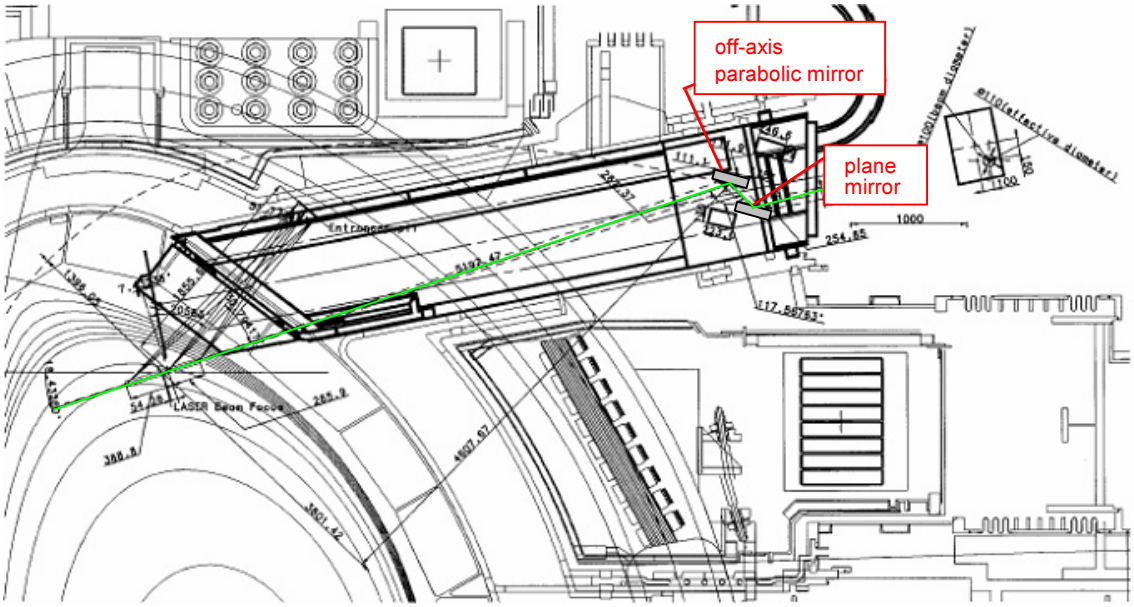


Fig. 2-1: Schematic view of the arrangement of the plane mirror and off-axis parabolic mirror for laser transmission.

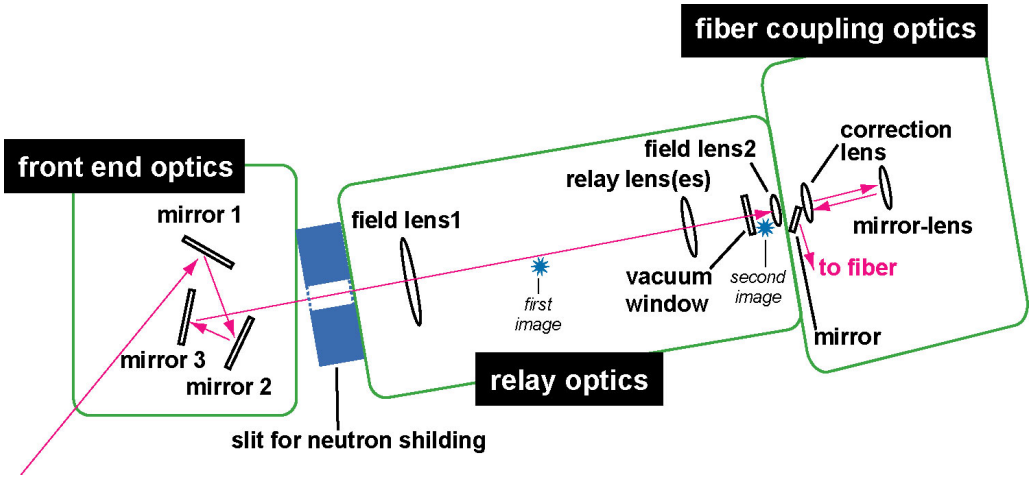


Fig. 2-2 Schematic diagram of the collection optical system consists of front-end optics, relay optics and fiber coupling optics.

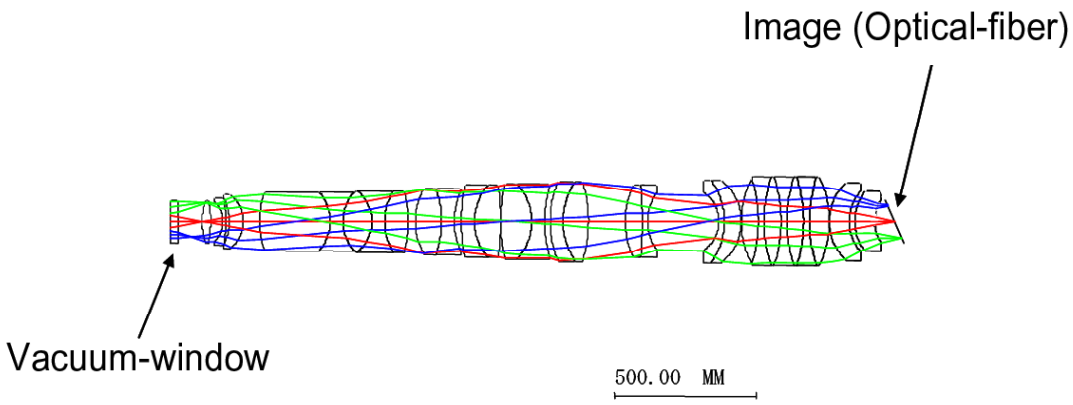


Fig. 3-1: Schematic of the optical arrangement for the refraction type system. The design has not been completed.

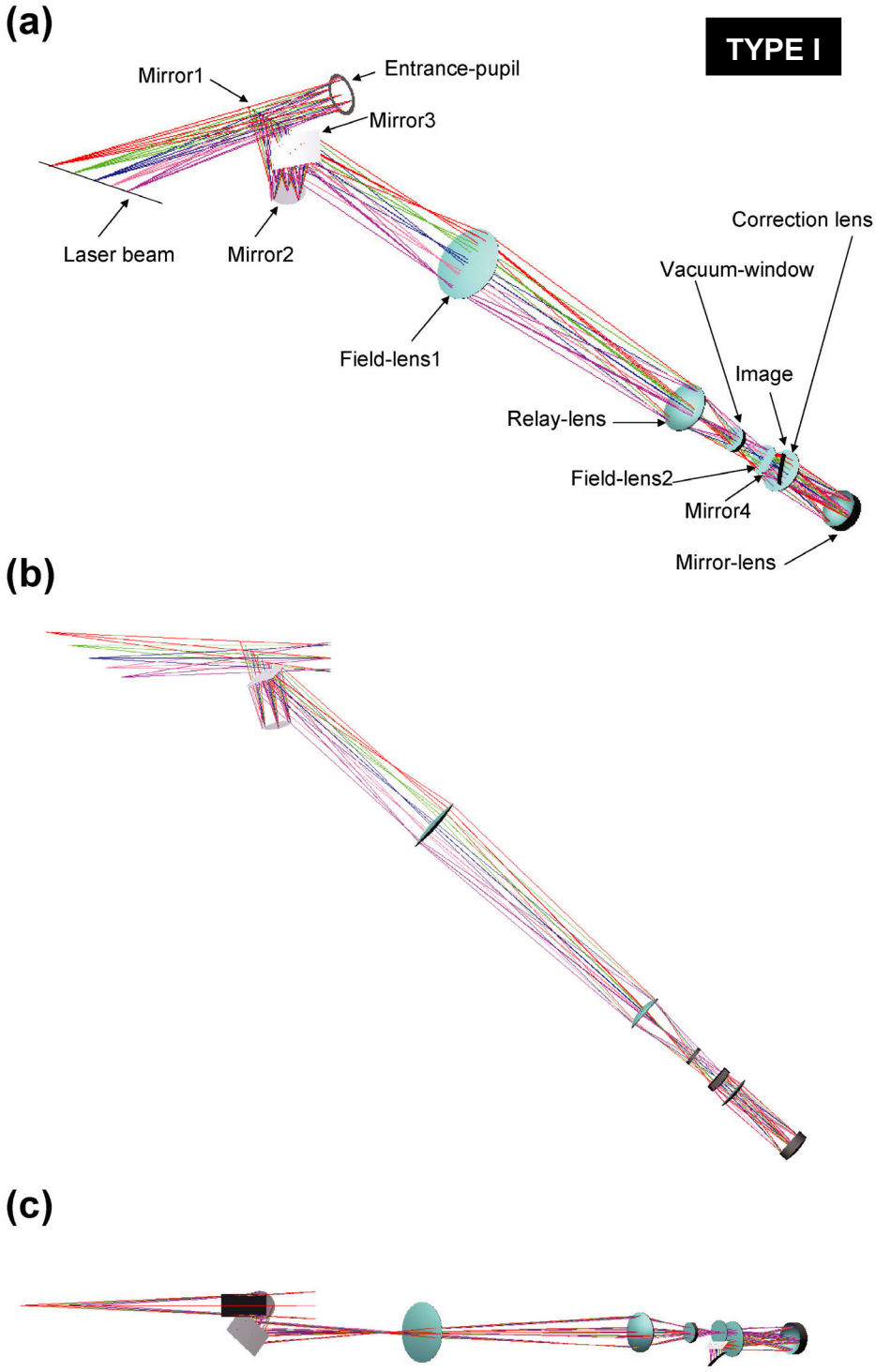


Fig. 3-2 Three-dimensional diagrams of the optical arrangement and ray path in Type-I arrangement from different eye views.

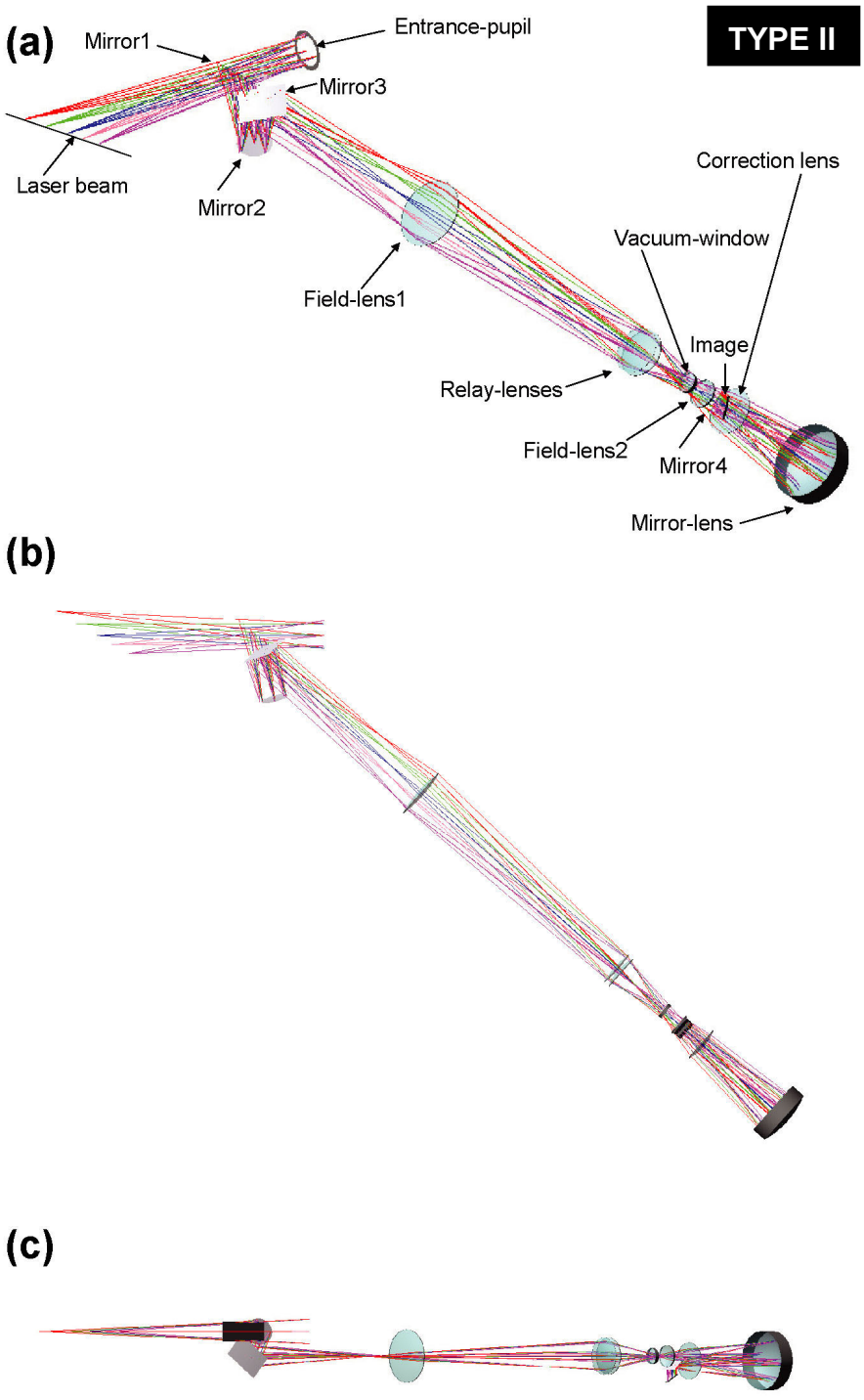


Fig. 3-3 Three-dimensional diagrams of the optical arrangement and ray path in Type-II arrangement from different eye views.

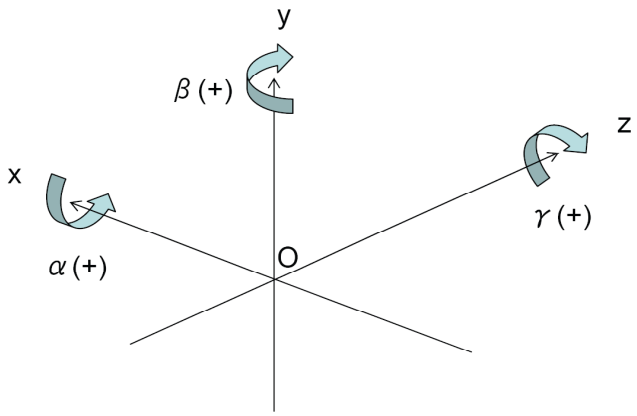


Fig. 4-1 The coordinates and the definition of the angle used in the analysis.

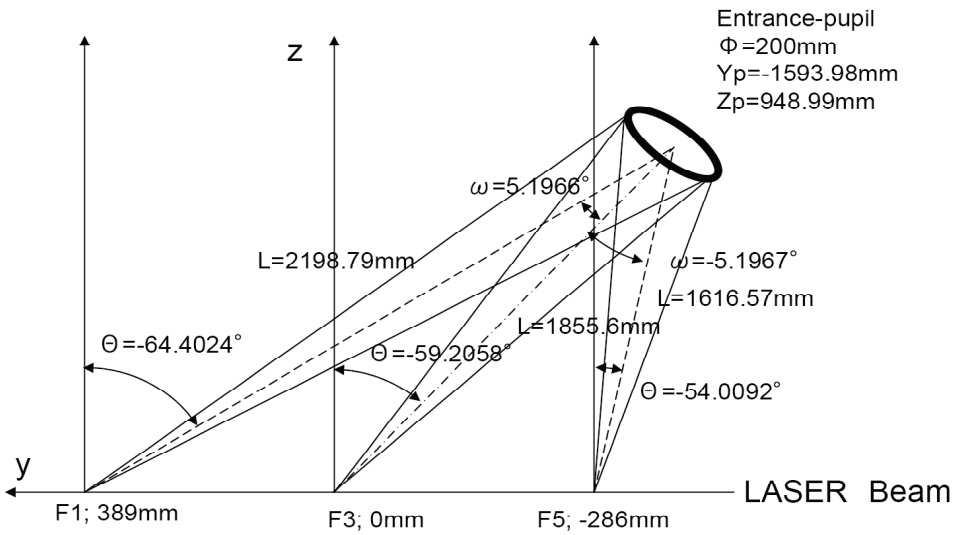


Fig. 4-2 Schematic diagram representing typical measurement points used for the analysis and the relation to the entrance pupil.

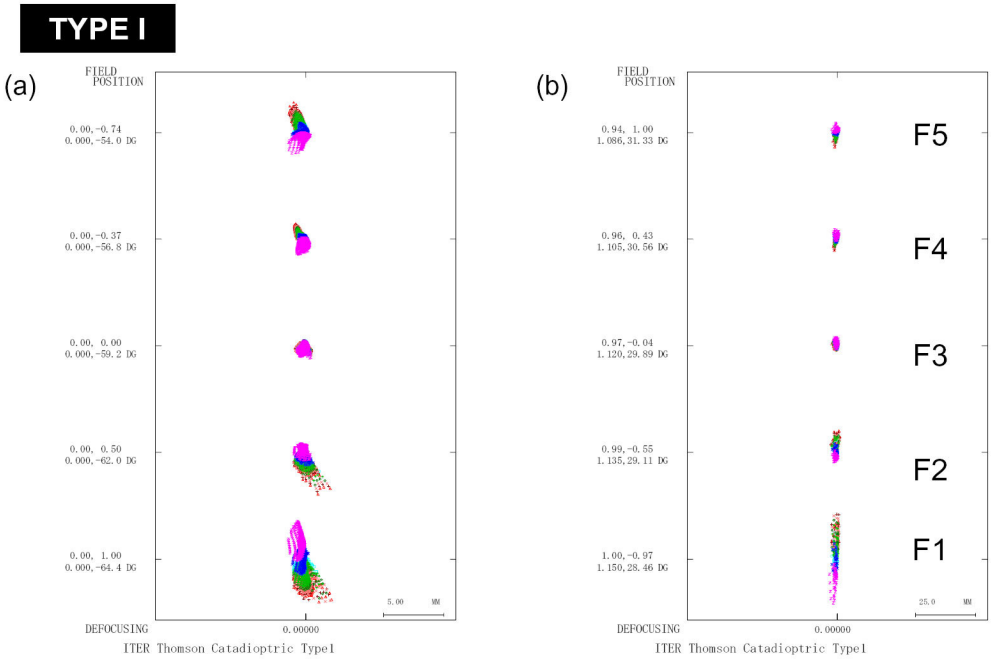


Fig. 4-3 Spot diagrams for the Type-I arrangement. (a) shows the image of the laser beam at the face of the fiber. (b) shows the image of the fiber at the laser beam position.

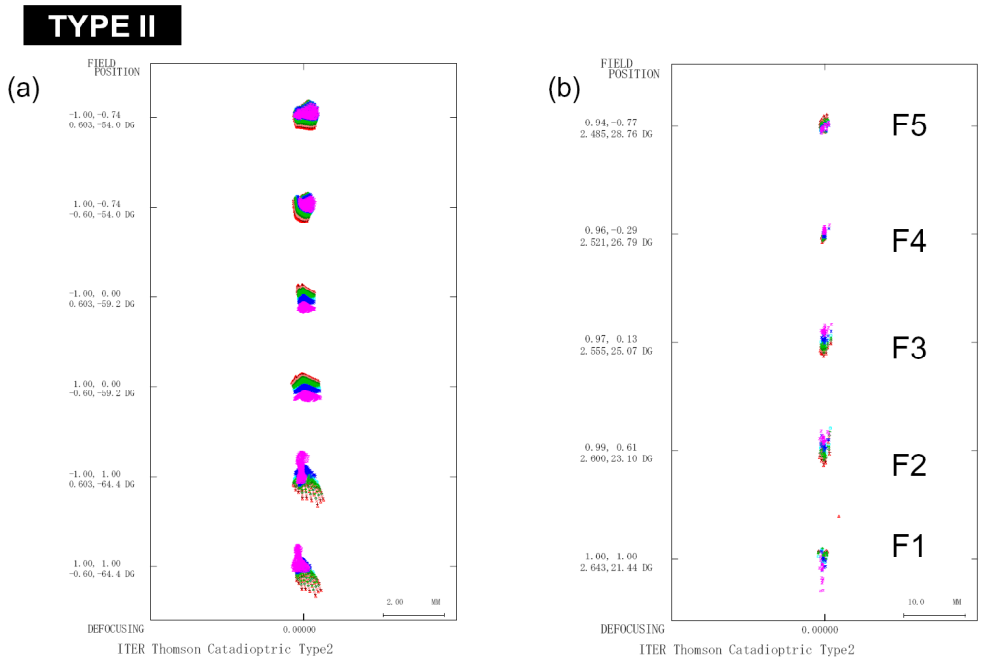


Fig. 4-4 Spot diagrams for the Type-II arrangement. (a) shows the image of the laser beam at the face of the fiber. (b) shows the image of the fiber at the laser beam position.

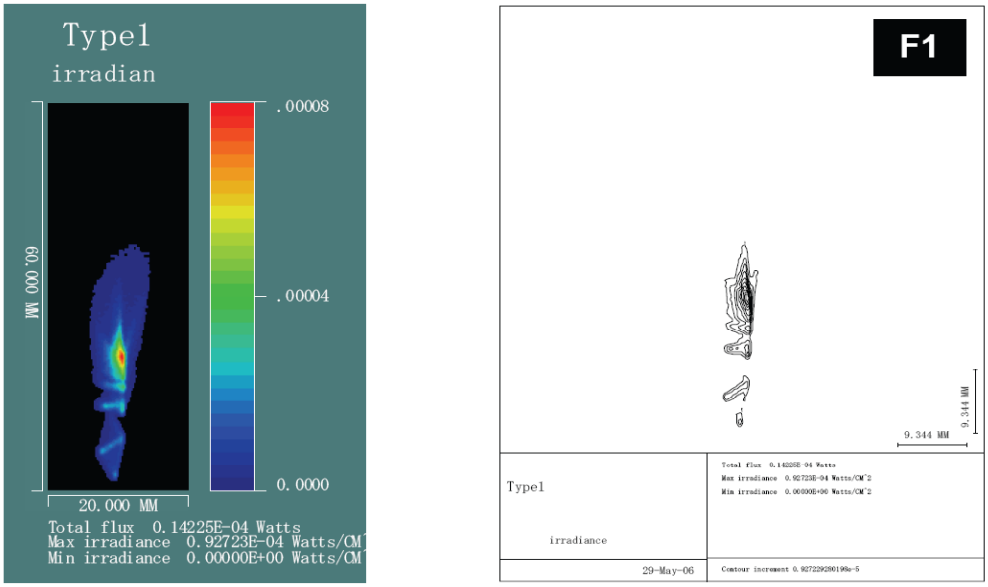


Fig. 4-5 Image plot and contour plot of the illumination profile from the fiber for the measurement point F1. The optics arrangement is Type-I.

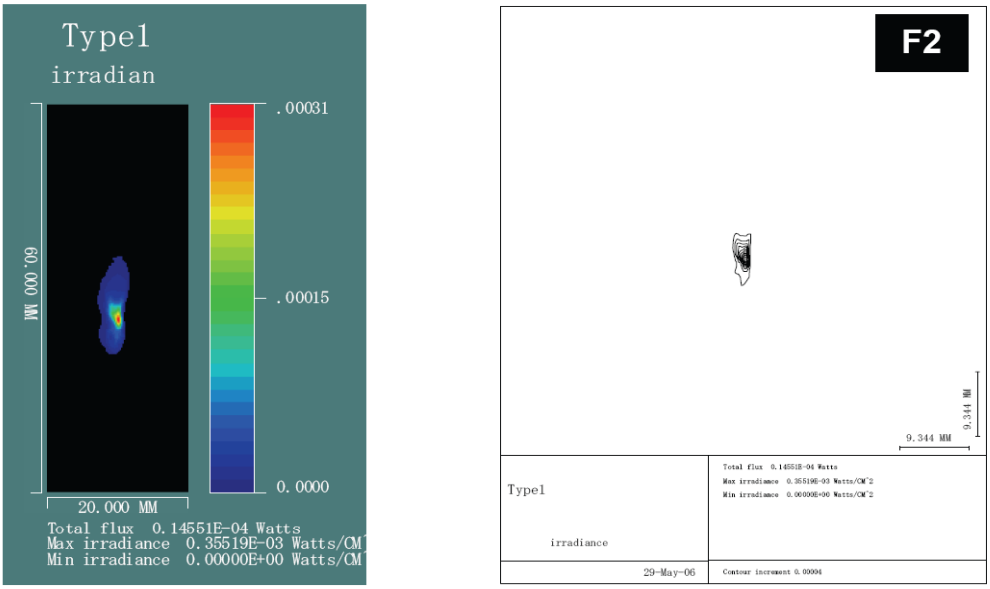


Fig. 4-6 Image plot and contour plot of the illumination profile from the fiber for the measurement point F2. The optics arrangement is Type-I.

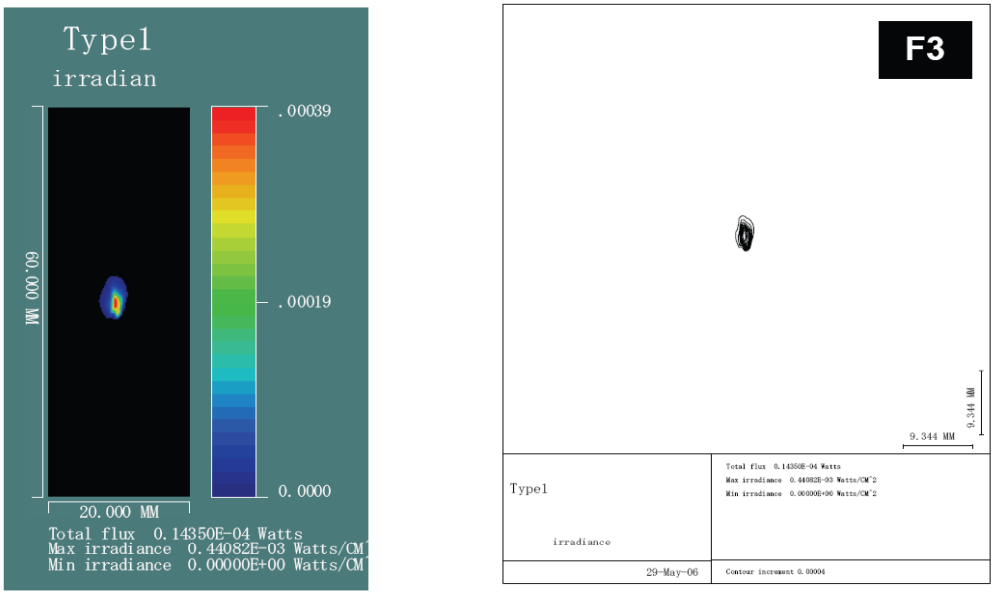


Fig. 4-7 Image plot and contour plot of the illumination profile from the fiber for the measurement point F3. The optics arrangement is Type-I.

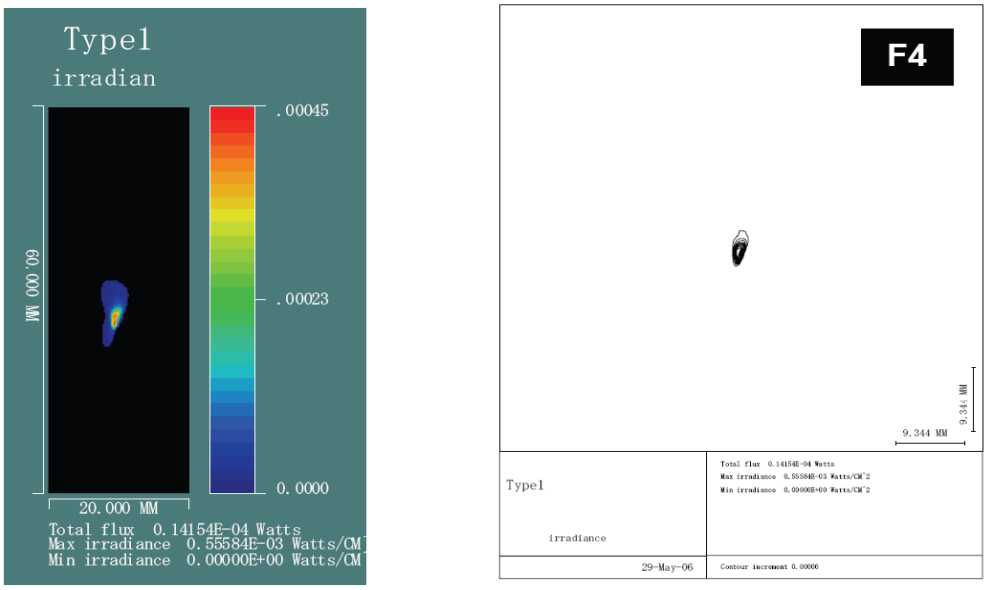


Fig. 4-8 Image plot and contour plot of the illumination profile from the fiber for the measurement point F4. The optics arrangement is Type-I.

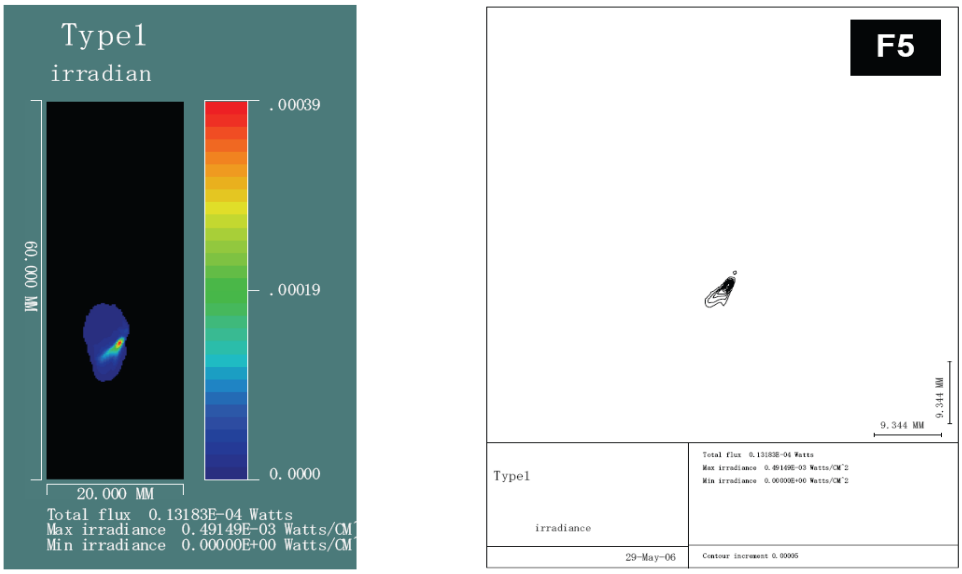


Fig. 4-9 Image plot and contour plot of the illumination profile from the fiber for the measurement point F5. The optics arrangement is Type-I.

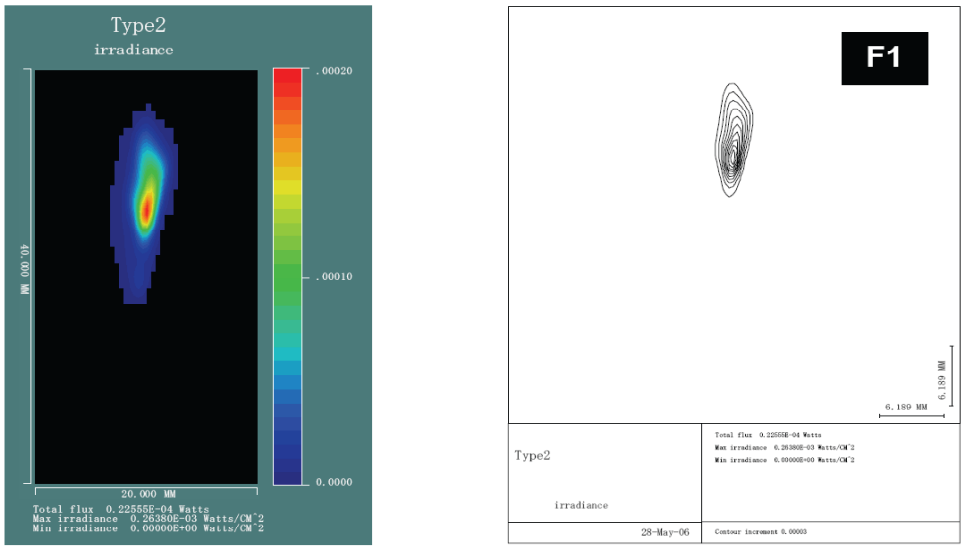


Fig. 4-10 Image plot and contour plot of the illumination profile from the fiber for the measurement point F1. The optics arrangement is Type-II.

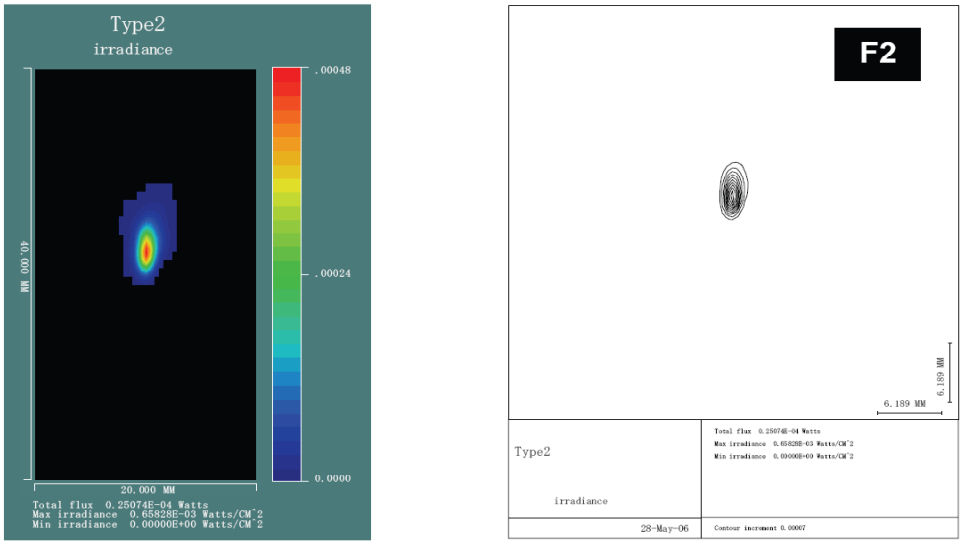


Fig. 4-11 Image plot and contour plot of the illumination profile from the fiber for the measurement point F2. The optics arrangement is Type-II.

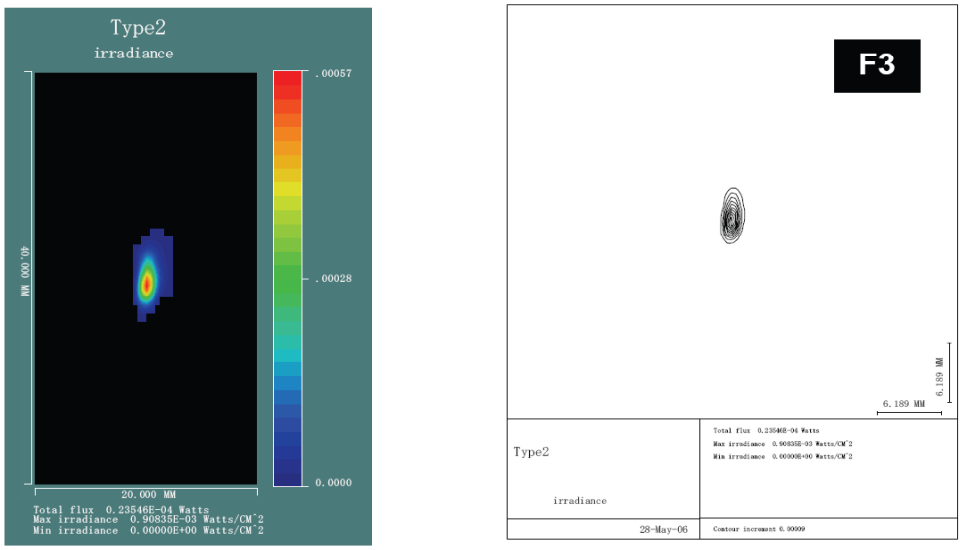


Fig. 4-12 Image plot and contour plot of the illumination profile from the fiber for the measurement point F3. The optics arrangement is Type-II.

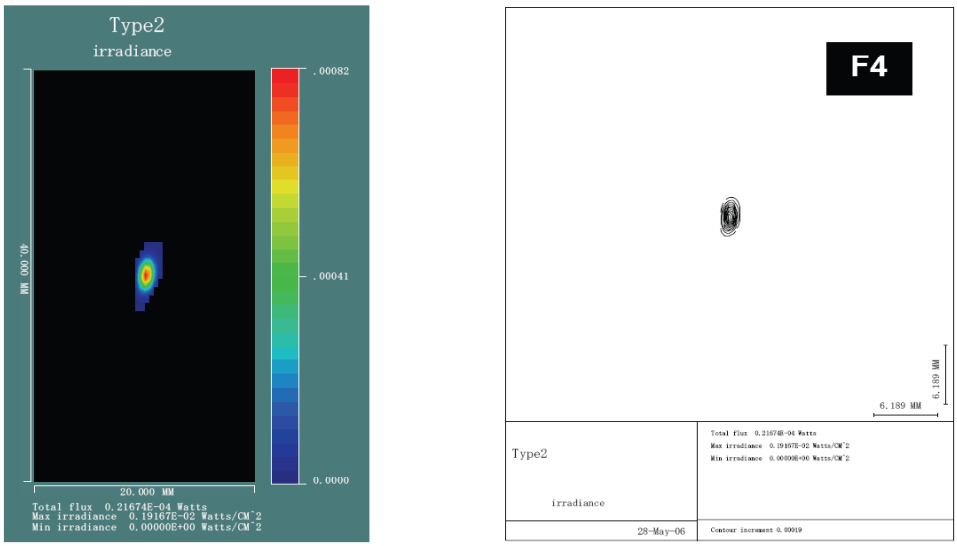


Fig. 4-13 Image plot and contour plot of the illumination profile from the fiber for the measurement point F4. The optics arrangement is Type-II.

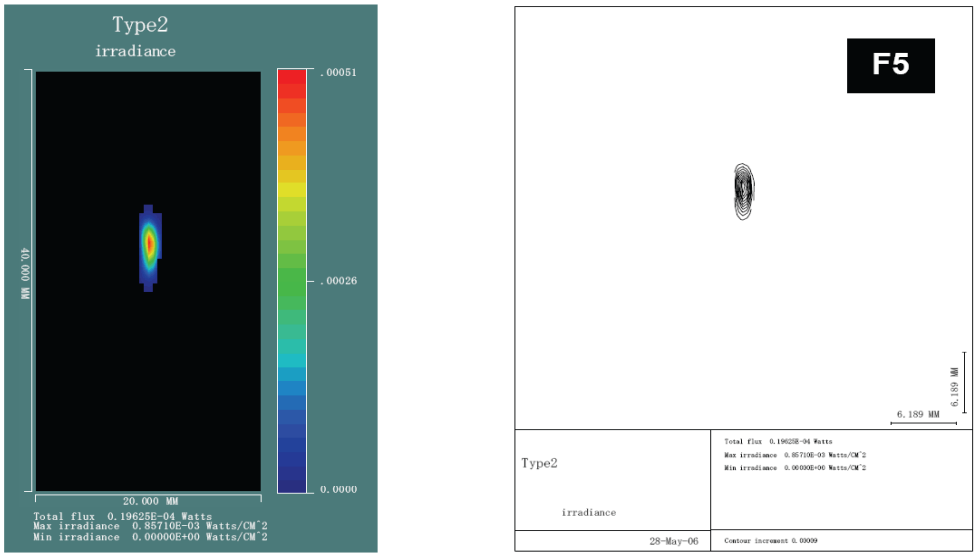


Fig. 4-14 Image plot and contour plot of the illumination profile from the fiber for the measurement point F5. The optics arrangement is Type-II.

## Appendix A. Data of the optical elements

Table A-1 The locations of the optical elements in Type-I with respect to the center position of the inner plane of the vacuum window port. The optical elements are presented as bold fonts in the name. The *z*-direction is the normal direction of the vacuum window port, *x*-direction is the horizontal direction, and the *y*-direction is the longitudinal direction. The order of the rotation is α, β, and γ.

Type-I

Local surface coordinates with respect to surface 35

| Name | Surface | XSC | YSC | ZSC | ASC | BSC | CSC |
|---|---|---|---|---|---|---|---|
| | OBJ | 200 | -475.3 | -5522.4 | 97.4324 | 0 | 0 |
| | 1 | 200 | -475.3 | -5522.4 | 38.2266 | 0 | 0 |
| stop | STO | 200 | 672.8942 | -4064.7 | 38.2266 | 0 | 0 |
| | 3 | 200 | -475.3 | -5522.4 | 97.4324 | 0 | 0 |
| | 4 | 200 | -475.3 | -5522.4 | 90 | 0 | 0 |
| | 5 | 200 | 105 | -5522.4 | 0 | 0 | 0 |
| front | 6 | 200 | 105 | -4769.4 | 0 | 0 | 0 |
| | 7 | 200 | 105 | -4769.4 | 0 | 0 | 0 |
| end | 8 | 200 | 105 | 0 | 0 | 0 | 0 |
| | 9 | 200 | 105 | -4769.4 | 0 | 0 | 0 |
| | 10 | 200 | 344.6 | -4481.6 | 0 | 0 | 0 |
| | 11 | 200 | 344.6 | -4481.6 | -90 | 0 | 0 |
| ***mirror1*** | 12 | 200 | 344.6 | -4481.6 | -90 | 0 | 0 |
| | 13 | 200 | 105 | -4769.4 | 0 | 0 | 0 |
| | 14 | 200 | 16.3 | -4064.7 | 0 | 0 | 0 |
| | 15 | 200 | 16.3 | -4064.7 | -38.2268 | -13.2833 | 0 |
| ***M2dev*** | 16 | 200 | 16.3 | -4064.7 | -38.2268 | -13.2833 | 0 |
| ***mirror2*** | 17 | 200 | 16.3 | -4064.7 | 141.7732 | 13.2833 | 50.7541 |
| | 18 | 200 | 105 | -4769.4 | 0 | 0 | 0 |
| | 19 | 0 | 263.8 | -4378.9 | 0 | 0 | 0 |
| | 20 | 0 | 263.8 | -4378.9 | -19.8651 | -13.8915 | 0 |
| ***M3dev*** | 21 | 0 | 263.8 | -4378.9 | -19.8651 | -13.8915 | 0 |
| ***mirror3*** | 22 | 0 | 263.8 | -4378.9 | 160.1349 | 13.8915 | 46.4721 |
| | 23 | 200 | 105 | -4769.4 | 0 | 0 | 0 |
| | 24 | 0 | 287.7 | -4769.4 | 0 | 0 | 0 |
| | 25 | 0 | 287.7 | -4769.4 | -3.5 | 0 | 0 |
| ***slit*** | 26 | 0 | 179.6441 | -3002.7 | 51.0721 | 0 | 0 |
| | 27 | 0 | 179.6441 | -3002.7 | -3.5 | 0 | 0 |
| ***FL1-s1*** | 28 | 0 | 159.4981 | -2673.32 | -3.5 | 0 | 0 |
| ***FL1-s2*** | 29 | 0 | 156.4456 | -2623.41 | -3.5 | 0 | 0 |
| | 30 | 0 | 179.6441 | -3002.7 | -3.5 | 0 | 0 |
| | 31 | 0 | 28.24371 | -527.327 | -3.5 | 0 | 0 |
| ***RL-s1*** | 32 | 0 | 28.24371 | -527.327 | -3.5 | 0 | 0 |
| ***RL-s2*** | 33 | 0 | 25.19128 | -477.42 | -3.5 | 0 | 0 |
| *View port* | 34 | 200 | 105 | 0 | 0 | 0 | 0 |
| ***window-s1*** | 35 | 0 | 0 | 0 | 0 | 0 | 0 |
| ***window-s2*** | 36 | 0 | 0 | 30 | 0 | 0 | 0 |
| | 37 | 0 | 28.24371 | -527.327 | -3.5 | 0 | 0 |
| ***FL2-s1*** | 38 | 0 | -22.4266 | 301.1248 | -3.5 | 0 | 0 |
| ***FL2-s2*** | 39 | 0 | -23.6476 | 321.0875 | -3.5 | 0 | 0 |
| ***FOL-s1f*** | 40 | -50 | -29.7524 | 420.901 | -3.5 | 0 | 0 |
| ***FOL-s2f*** | 41 | -50 | -31.8891 | 455.8357 | -3.5 | 0 | 0 |
| ***FOM-s1f*** | 42 | -45 | -66.522 | 1054.839 | -3.5 | 0 | 0 |
| ***FOM-s2s*** | 43 | -45 | -68.9639 | 1094.764 | -3.5 | 0 | 0 |
| ***FOM-s1s*** | 44 | -45 | -66.522 | 1054.839 | -3.5 | 0 | 0 |
| ***FOL-s2s*** | 45 | -50 | -31.8891 | 455.8357 | -3.5 | 0 | 0 |
| ***FOL-s1s*** | 46 | -50 | -29.7524 | 420.901 | -3.5 | 0 | 0 |
| ***mirror4*** | 47 | -50 | -23.6476 | 321.0875 | -3.5 | 45 | 0 |
| | 48 | -191.65 | -23.6476 | 321.0875 | 86.5 | 60.0612 | -90 |
| | IMG | -191.65 | -23.6476 | 321.0875 | 86.5 | 60.0612 | -90 |

Table A-2 The locations of the optical elements in Type-II with respect to the center position of the inner plane of the vacuum window port. The optical elements are presented as bold fonts in the name. The *z*-direction is the normal direction of the vacuum window port, *x*-direction is the horizontal direction, and the *y*-direction is the longitudinal direction. The order of the rotation is α, β, and γ.

Type-II

Local surface coordinates with respect to surface 38

| Name | Surface | XSC | YSC | ZSC | ASC | BSC | CSC |
|---|---|---|---|---|---|---|---|
| | OBJ | 200 | -475.3 | -5522.4 | 97.4324 | 0 | 0 |
| | 1 | 200 | -475.3 | -5522.4 | 38.2266 | 0 | 0 |
| stop | STO | 200 | 672.89422 | -4064.69585 | 38.2266 | 0 | 0 |
| | 3 | 200 | -475.3 | -5522.4 | 97.4324 | 0 | 0 |
| | 4 | 200 | -475.3 | -5522.4 | 90 | 0 | 0 |
| | 5 | 200 | 105 | -5522.4 | 0 | 0 | 0 |
| front | 6 | 200 | 105 | -4769.4 | 0 | 0 | 0 |
| | 7 | 200 | 105 | -4769.4 | 0 | 0 | 0 |
| end | 8 | 200 | 105 | 0 | 0 | 0 | 0 |
| | 9 | 200 | 105 | -4769.4 | 0 | 0 | 0 |
| | 10 | 200 | 344.6 | -4481.6 | 0 | 0 | 0 |
| | 11 | 200 | 344.6 | -4481.6 | -90 | 0 | 0 |
| ***mirror1*** | 12 | 200 | 344.6 | -4481.6 | -90 | 0 | 0 |
| | 13 | 200 | 105 | -4769.4 | 0 | 0 | 0 |
| | 14 | 200 | 16.3 | -4064.7 | 0 | 0 | 0 |
| | 15 | 200 | 16.3 | -4064.7 | -38.2268 | -13.2833 | 0 |
| ***M2dev*** | 16 | 200 | 16.3 | -4064.7 | -38.2268 | -13.2833 | 0 |
| ***mirror2*** | 17 | 200 | 16.3 | -4064.7 | 141.7732 | 13.2833 | 50.7541 |
| | 18 | 200 | 105 | -4769.4 | 0 | 0 | 0 |
| | 19 | 0 | 263.8 | -4378.9 | 0 | 0 | 0 |
| | 20 | 0 | 263.8 | -4378.9 | -19.8651 | -13.8915 | 0 |
| ***M3dev*** | 21 | 0 | 263.8 | -4378.9 | -19.8651 | -13.8915 | 0 |
| ***mirror3*** | 22 | 0 | 263.8 | -4378.9 | 160.1349 | 13.8915 | 46.4721 |
| | 23 | 200 | 105 | -4769.4 | 0 | 0 | 0 |
| | 24 | 0 | 287.7 | -4769.4 | 0 | 0 | 0 |
| | 25 | 0 | 287.7 | -4769.4 | -3.5 | 0 | 0 |
| ***slit*** | 26 | 0 | 179.64409 | -3002.70141 | 51.0721 | 0 | 0 |
| | 27 | 0 | 179.64409 | -3002.70141 | -3.5 | 0 | 0 |
| ***FL1-s1*** | 28 | 0 | 159.49807 | -2673.31692 | -3.5 | 0 | 0 |
| ***FL1-s2*** | 29 | 0 | 156.44564 | -2623.41018 | -3.5 | 0 | 0 |
| | 30 | 0 | 179.64409 | -3002.70141 | -3.5 | 0 | 0 |
| | 31 | 0 | 28.24371 | -527.32711 | -3.5 | 0 | 0 |
| ***RL-s1*** | 32 | 0 | 26.10701 | -492.39239 | -3.5 | 0 | 0 |
| ***RL-s2*** | 33 | 0 | 25.98491 | -490.39612 | -3.5 | 0 | 0 |
| *View port* | 34 | 0 | 24.4587 | -465.44275 | -3.5 | 0 | 0 |
| ***window-s1*** | 35 | 0 | 179.64409 | -3002.70141 | -3.5 | 0 | 0 |
| ***window-s2*** | 36 | 0 | 24.4587 | -465.44275 | -3.5 | 0 | 0 |
| | 37 | 200 | 105 | 0 | 0 | 0 | 0 |
| ***FL2-s1*** | 38 | 0 | 0 | 0 | 0 | 0 | 0 |
| ***FL2-s2*** | 39 | 0 | 0 | 30 | 0 | 0 | 0 |
| ***FOL-s1f*** | 40 | 0 | 24.4587 | -465.44275 | -3.5 | 0 | 0 |
| ***FOL-s2f*** | 41 | 0 | -15.77229 | 192.32808 | -3.5 | 0 | 0 |
| ***FOM-s1f*** | 42 | 0 | -17.2985 | 217.28145 | -3.5 | 0 | 0 |
| ***FOM-s2s*** | 43 | -40 | -29.50821 | 416.90841 | -3.5 | 0 | 0 |
| ***FOM-s1s*** | 44 | -40 | -31.33967 | 446.85246 | -3.5 | 0 | 0 |
| ***FOL-s2s*** | 45 | -36 | -77.04249 | 1295.64554 | -3.5 | 0 | 0 |
| ***FOL-s1s*** | 46 | -36 | -81.01065 | 1360.5243 | -3.5 | 0 | 0 |
| ***mirror4*** | 47 | -36 | -77.04249 | 1295.64554 | -3.5 | 0 | 0 |
| | 48 | -40 | -31.33967 | 446.85246 | -3.5 | 0 | 0 |
| | IMG | -40 | -29.50821 | 416.90841 | -3.5 | 0 | 0 |

Followings are the lens data in CODE-V[10] format. The order of the rotational eccentricity is $\alpha$, $\beta$, and $\gamma$.

LASER

```
        ITER Thomson LASER Type1
                    RDY                 THI        RMD          GLA              CCY     THC     GLC
> OBJ:              INFINITY            INFINITY                                  100     100
   STO:             INFINITY            254.850000                                100     100
     2:             INFINITY            -287.370000    REFL                       100     100
       SLB: "plane"
       XDE:         0.000000     YDE:      0.000000     ZDE:      0.000000     BEN
       XDC:         100          YDC:      100          ZDC:      100
       ADE:        62.500000     BDE:      0.000000     CDE:      0.000000
       ADC:         100          BDC:      100          CDC:      100

     3:             INFINITY            -3801.420000                              100     100
       XDE:         0.000000     YDE:-4607.371500     ZDE:      0.000000
       XDC:         100          YDC:      100          ZDC:      100
       ADE:         0.000000     BDE:      0.000000     CDE:      0.000000
       ADC:         100          BDC:      100          CDC:      100
       XOD:         0.000000     YOD:      0.000000     ZOD:      0.000000
       XOC:         100          YOC:      100          ZOC:      100

     4:          2792.10376              0.000000    REFL                       100     100
       SLB: "parabola"
       ASP:
       K    :     -1.000000     KC :         100
       IC :         YES          CUF:      0.000000     CCF:         100
       A    :0.000000E+00     B    :0.000000E+00     C    :0.000000E+00     D    :0.000000E+00
       AC :         100          BC :         100          CC :         100          DC :         100

     5:             INFINITY            1396.051880                               100     100
     6:             INFINITY            -5197.458920                              100     100
       XDE:         0.000000     YDE:      0.000000     ZDE:      0.000000
       XDC:         100          YDC:      100          ZDC:      100
       ADE:        62.432357     BDE:      0.000000     CDE:      0.000000
       ADC:         100          BDC:      100          CDC:      100

     7:             INFINITY            5197.458920                               100     100
     8:             INFINITY            0.000000           SIO2_SCHOTT            100     100
       SLB: "focus"
     9:             INFINITY            500.000000                                100     100
    10:             INFINITY            -500.000000                               100     PIM
   IMG:             INFINITY            0.000000                                  100     100

SPECIFICATION DATA
    EPD          100.00000
    DIM                MM
    WL             1064.00
    REF                1
    WTW                1
    XAN            0.00000
```

| | |
|---|---|
| YAN | 0.00000 |
| WTF | 1.00000 |
| VUX | 0.00000 |
| VLX | 0.00000 |
| VUY | 0.00000 |
| VLY | 0.00000 |
| POL | N |

APERTURE DATA/EDGE DEFINITIONS

| | |
|---|---|
| CA | |
| REX S2 | 65.000000 |
| REY S2 | 123.300000 |
| REX S4 | 65.000000 |
| REY S4 | 57.800000 |
| ADY S4 | 4607.600000 |
| CIR S8 | 20.000000 |

REFRACTIVE INDICES

| | |
|---|---|
| GLASS CODE | 1064.00 |
| SIO2_SCHOTT | 1.449604 |

SOLVES

PIM

No pickups defined in system

This is a non-symmetric system. If elements with power are decentered or tilted, the first order properties are probably inadequate in describing the system characteristics.

INFINITE CONJUGATES

| | |
|---|---|
| EFL | 1396.0519 |
| BFL | -500.0000 |
| FFL | 2947.5881 |
| FNO | 13.9605 |
| IMG DIS | -500.0000 |
| OAL | -1937.8881 |
| PARAXIAL IMAGE | |
| HT | 0.0000 |
| ANG | 0.0000 |
| ENTRANCE PUPIL | |
| DIA | 100.0000 |
| THI | 0.0000 |
| EXIT PUPIL | |
| DIA | 47.3625 |
| THI | 161.2053 |

Type-I

ITER Thomson Catadioptric Type1

| | RDY | THI | RMD | GLA | CCY | THC | GLC |
|---|---|---|---|---|---|---|---|
| OBJ: | INFINITY | 0.000000 | | | 100 | 100 | |
| 1: | INFINITY | 1855.600000 | | | 100 | 100 | |
| XDE: | 0.000000 | YDE: 0.000000 | ZDE: | 0.000000 | | | |
| XDC: | 100 | YDC: 100 | ZDC: | 100 | | | |
| ADE: | -59.205830 | BDE: 0.000000 | CDE: | 0.000000 | | | |
| ADC: | 100 | BDC: 100 | CDC: | 100 | | | |
| STO: | INFINITY | -1855.600000 | | | 100 | 100 | |
| 3: | INFINITY | 0.000000 | | | 100 | 100 | |
| RET | S0 | | | | | | |
| 4: | INFINITY | 580.300000 | | | 100 | 100 | |
| XDE: | 0.000000 | YDE: 0.000000 | ZDE: | 0.000000 | | | |
| XDC: | 100 | YDC: 100 | ZDC: | 100 | | | |
| ADE: | -7.432380 | BDE: 0.000000 | CDE: | 0.000000 | | | |
| ADC: | 100 | BDC: 100 | CDC: | 100 | | | |
| 5: | INFINITY | 753.000000 | | | 100 | 100 | |
| XDE: | 0.000000 | YDE: 0.000000 | ZDE: | 0.000000 | | | |
| XDC: | 100 | YDC: 100 | ZDC: | 100 | | | |
| ADE: | -90.000000 | BDE: 0.000000 | CDE: | 0.000000 | | | |
| ADC: | 100 | BDC: 100 | CDC: | 100 | | | |
| 6: | INFINITY | 0.000000 | | | 100 | 100 | |
| SLB: "front" | | | | | | | |
| 7: | INFINITY | 4769.400000 | | | 100 | 100 | |
| 8: | INFINITY | 0.000000 | | | 100 | 100 | |
| SLB: "end" | | | | | | | |
| 9: | INFINITY | 287.800000 | | | 100 | 100 | |
| RET | S6 | | | | | | |
| 10: | INFINITY | 0.000000 | | | 100 | 100 | |
| XDE: | 0.000000 | YDE: 239.600000 | ZDE: | 0.000000 | | | |
| XDC: | 100 | YDC: 100 | ZDC: | 100 | | | |
| ADE: | 0.000000 | BDE: 0.000000 | CDE: | 0.000000 | | | |
| ADC: | 100 | BDC: 100 | CDC: | 100 | | | |
| 11: | INFINITY | 0.000000 | | | 100 | 100 | |
| XDE: | 0.000000 | YDE: 0.000000 | ZDE: | 0.000000 | | | |
| XDC: | 100 | YDC: 100 | ZDC: | 100 | | | |
| ADE: | -90.000000 | BDE: 0.000000 | CDE: | 0.000000 | | | |
| ADC: | 100 | BDC: 100 | CDC: | 100 | | | |
| 12: | INFINITY | 0.000000 | REFL | | 100 | 100 | |
| SLB: "mirror1" | | | | | | | |
| 13: | INFINITY | 704.700000 | | | 100 | 100 | |
| RET | S6 | | | | | | |
| 14: | INFINITY | 0.000000 | | | 100 | 100 | |
| XDE: | 0.000000 | YDE: -88.700000 | ZDE: | 0.000000 | | | |

```
    XDC:        100         YDC:        100         ZDC:        100
    ADE:      0.000000      BDE:      0.000000      CDE:      0.000000
    ADC:        100         BDC:        100         CDC:        100

15:           INFINITY          0.000000                          100     100
    XDE:      0.000000      YDE:      0.000000      ZDE:      0.000000
    XDC:        100         YDC:        100         ZDC:        100
    ADE:    -38.226767      BDE:    -13.283317      CDE:      0.000000
    ADC:        100         BDC:        100         CDC:        100

16:           INFINITY          0.000000                          100     100
    SLB: "M2dev"
    XDE:      0.000000      YDE:      0.000000      ZDE:      0.000000
    XDC:        100         YDC:        100         ZDC:        100
    ADE:      0.000000      BDE:      0.000000      CDE:      0.000000
    ADC:        100         BDC:        100         CDC:        100

17:        1855.60000           0.000000    REFL                  100     100
    SLB: "mirror2"
    XTO:
    RDX:    3261.30568      CCX:        100
    K    :      0.000000     KC :        100          IC :        YES
    A    :0.000000E+00       B    :0.000000E+00       C    :0.000000E+00       D    :0.000000E+00
    AC :        100          BC :        100          CC :        100          DC :        100
    XDE:      0.000000      YDE:      0.000000      ZDE:      0.000000
    XDC:        100         YDC:        100         ZDC:        100
    ADE:    180.000000      BDE:      0.000000      CDE:     50.754088
    ADC:        100         BDC:        100         CDC:        100

18:           INFINITY        390.500000                          100     100
    RET         S6

19:           INFINITY          0.000000                          100     100
    XDE: -200.000000      YDE:    158.800000      ZDE:      0.000000
    XDC:        100         YDC:        100         ZDC:        100
    ADE:      0.000000      BDE:      0.000000      CDE:      0.000000
    ADC:        100         BDC:        100         CDC:        100

20:           INFINITY          0.000000                          100     100
    XDE:      0.000000      YDE:      0.000000      ZDE:      0.000000
    XDC:        100         YDC:        100         ZDC:        100
    ADE:    -19.865095      BDE:    -13.891460      CDE:      0.000000
    ADC:        100         BDC:        100         CDC:        100

21:           INFINITY          0.000000                          100     100
    SLB: "M3dev"
    XDE:      0.000000      YDE:      0.000000      ZDE:      0.000000
    XDC:        100         YDC:        100         ZDC:        100
    ADE:      0.000000      BDE:      0.000000      CDE:      0.000000
    ADC:        100         BDC:        100         CDC:        100

22:           INFINITY          0.000000    REFL                  100     100
    SLB: "mirror3"
    XTO:
```

```
      RDX: -3295.75965    CCX:        100
      K   :    0.000000   KC :        100          IC :        YES
      A   :0.000000E+00   B  :0.000000E+00   C  :0.000000E+00   D  :0.000000E+00
      AC :        100     BC :        100     CC :        100     DC :        100
      XDE:    0.000000    YDE:    0.000000    ZDE:    0.000000
      XDC:        100     YDC:        100     ZDC:        100
      ADE:  180.000000    BDE:    0.000000    CDE:   46.472120
      ADC:        100     BDC:        100     CDC:        100

   23:           INFINITY          0.000000                          100     100
      RET       S6

   24:           INFINITY          0.000000                          100     100
      XDE: -200.000000    YDE:  182.700000    ZDE:    0.000000
      XDC:        100     YDC:        100     ZDC:        100
      ADE:    0.000000    BDE:    0.000000    CDE:    0.000000
      ADC:        100     BDC:        100     CDC:        100

   25:           INFINITY       1770.000000                          100     100
      XDE:    0.000000    YDE:    0.000000    ZDE:    0.000000
      XDC:        100     YDC:        100     ZDC:        100
      ADE:   -3.500000    BDE:    0.000000    CDE:    0.000000
      ADC:        100     BDC:        100     CDC:        100

   26:           INFINITY          0.000000                          100     100
      SLB: "slit"
      XDE:    0.000000    YDE:    0.000000    ZDE:    0.000000    DAR
      XDC:        100     YDC:        100     ZDC:        100
      ADE:   54.572100    BDE:    0.000000    CDE:    0.000000
      ADC:        100     BDC:        100     CDC:        100

   27:           INFINITY        330.000000                          100     100
   28:         1100.00000         50.000000         SIO2_SCHOTT       100     100
      SLB: "FL1-s1"
   29:        -1100.00000          0.000000                          100     100
      SLB: "FL1-s2"
   30:           INFINITY       2480.000000                          100     100
      RET       S27

   31:           INFINITY          0.000000                          100     100
   32:          285.00000         50.000000         SIO2_SCHOTT       100     100
      SLB: "RL-s1"
   33:           INFINITY          0.000000                          100     100
      SLB: "RL-s2"
   34:           INFINITY          0.000000                          100     100
      RET       S8

>  35:           INFINITY         30.000000         SIO2_SCHOTT       100     100
      SLB: "window-s1"
      XDE: -200.000000    YDE: -105.000000    ZDE:    0.000000
      XDC:        100     YDC:        100     ZDC:        100
      ADE:    0.000000    BDE:    0.000000    CDE:    0.000000
      ADC:        100     BDC:        100     CDC:        100
```

```
36:            INFINITY          0.000000                              100     100
    SLB: "window-s2"
37:            INFINITY        830.000000                              100     100
    RET        S31

38:            INFINITY         20.000000          SIO2_SCHOTT          100     100
    SLB: "FL2-s1"
39:         -306.85234         100.000000                              100     100
    SLB: "FL2-s2"
40:         1136.43754          35.000000          SIO2_SCHOTT          100     100
    SLB: "FOL-s1f"
    XDE:   -50.000000    YDE:      0.000000    ZDE:      0.000000
    XDC:        100      YDC:       100        ZDC:       100
    ADE:      0.000000   BDE:      0.000000    CDE:      0.000000
    ADC:        100      BDC:       100        CDC:       100

41:         -453.32524         600.000000                              100     100
    SLB: "FOL-s2f"
42:         -161.75048          40.000000          SIO2_SCHOTT          100     100
    SLB: "FOM-s1f"
    XDE:      5.000000   YDE:      2.000000    ZDE:      0.000000
    XDC:        100      YDC:       100        ZDC:       100
    ADE:      0.000000   BDE:      0.000000    CDE:      0.000000
    ADC:        100      BDC:       100        CDC:       100

43:         -405.14902         -40.000000   REFL SIO2_SCHOTT          100     100
    SLB: "FOM-s2s"
44:         -161.75048        -600.000000                              100     100
    SLB: "FOM-s1s"
45:         -453.32524         -35.000000          SIO2_SCHOTT          100     100
    SLB: "FOL-s2s"
    RET        S41

46:         1136.43754        -100.000000                              100     100
    SLB: "FOL-s1s"
47:            INFINITY        141.650000   REFL                        100     100
    SLB: "mirror4"
    XDE:      0.000000   YDE:      0.000000    ZDE:      0.000000    BEN
    XDC:        100      YDC:       100        ZDC:       100
    ADE:      0.000000   BDE:     45.000000    CDE:      0.000000
    ADC:        100      BDC:       100        CDC:       100

48:            INFINITY          0.000000                              100     100
    XDE:      0.000000   YDE:      0.000000    ZDE:      0.000000
    XDC:        100      YDC:       100        ZDC:       100
    ADE:     29.938803   BDE:      0.000000    CDE:      0.000000
    ADC:        100      BDC:       100        CDC:       100

IMG:         663.12479          0.000000                              100     100
    CYL:
    RDX:      INFINITY    CCX:       100
```

SPECIFICATION DATA

| | | | | | | | |
|---|---|---|---|---|---|---|---|
| EPD | 200.00000 | | | | | | |
| DIM | MM | | | | | | |
| WL | 1100.00 | 1000.00 | 900.00 | 800.00 | 700.00 | 600.00 | 500.00 |
| | 400.00 | | | | | | |
| REF | 6 | | | | | | |
| WTW | 1 | 1 | 1 | 1 | 1 | 1 | 1 |
| | 1 | | | | | | |
| XOB | 0.00000 | 0.00000 | 0.00000 | 0.00000 | 0.00000 | | |
| YOB | 389.00000 | 194.50000 | 0.00000 | -143.00000 | -286.00000 | | |
| WTF | 1.00000 | 1.00000 | 1.00000 | 1.00000 | 1.00000 | | |
| VUX | -0.95329 | -0.95329 | -0.95329 | -0.95329 | -0.95329 | | |
| VLX | -0.95329 | -0.95329 | -0.95329 | -0.95329 | -0.95329 | | |
| VUY | -3.12906 | -2.81402 | -2.49897 | -2.26734 | -2.03571 | | |
| VLY | -3.95003 | -3.57234 | -3.19466 | -2.91698 | -2.63929 | | |
| POL | N | | | | | | |

APERTURE DATA/EDGE DEFINITIONS

| | |
|---|---|
| CA | |
| CIR S2 | 100.000000 |
| REX S12 | 85.000000 |
| REY S12 | 215.000000 |
| CIR S17 | 110.000000 |
| REX S22 | 150.000000 |
| REY S22 | 112.500000 |
| ADY S22 | 2.500000 |
| CIR S28 | 225.000000 |
| CIR S29 | 225.000000 |
| CIR S32 | 150.000000 |
| CIR S33 | 150.000000 |
| CIR S35 | 75.000000 |
| CIR S36 | 75.000000 |
| CIR S38 | 92.500000 |
| CIR S39 | 92.500000 |
| CIR S40 | 132.000000 |
| CIR S41 | 132.000000 |
| CIR S42 | 117.000000 |
| CIR S43 | 130.000000 |
| CIR S44 | 117.000000 |
| CIR S45 | 135.000000 |
| CIR S46 | 135.000000 |
| REX S47 | 40.000000 |
| REY S47 | 100.000000 |
| ADX S47 | -59.700000 |
| REX S49 | 20.000000 |
| REY S49 | 100.000000 |
| ADX S49 | -39.700000 |

REFRACTIVE INDICES

| GLASS CODE | 1100.00 | 1000.00 | 900.00 | 800.00 | 700.00 | 600.00 | 500.00 |
|---|---|---|---|---|---|---|---|
| | 400.00 | | | | | | |
| SIO2_SCHOTT | 1.449177 | 1.450390 | 1.451725 | 1.453288 | 1.455263 | 1.458009 | 1.462299 |
| | 1.470094 | | | | | | |

No solves defined in system

No pickups defined in system

This is a non-symmetric system. If elements with power are decentered or tilted, the first order properties are probably inadequate in describing the system characteristics.

| | |
|---|---|
| INFINITE CONJUGATES | |
| EFL | -1755.4904 |
| BFL | -1669.0133 |
| FFL | -1655.1257 |
| FNO | 8.7775 |
| AT USED CONJUGATES | |
| RED | -1.0606 |
| FNO | -9.8549 |
| OBJ DIS | 0.0000 |
| TT | 9040.1985 |
| IMG DIS | 0.0000 |
| OAL | 9040.1985 |
| PARAXIAL IMAGE | |
| HT | 303.3427 |
| THI | 192.9278 |
| ANG | 54.0092 |
| ENTRANCE PUPIL | |
| DIA | 200.0000 |
| THI | 1855.6000 |
| EXIT PUPIL | |
| DIA | 100.0073 |
| THI | -791.2043 |

Type2

```
ITER Thomson Catadioptric Type2
                RDY             THI       RMD        GLA            CCY   THC   GLC
OBJ:          INFINITY        0.000000                              100   100
  1:          INFINITY     1855.600000                              100   100
    XDE:      0.000000   YDE:  0.000000   ZDE:      0.000000
    XDC:       100       YDC:   100       ZDC:       100
    ADE:   -59.205830    BDE:  0.000000   CDE:      0.000000
    ADC:       100       BDC:   100       CDC:       100

STO:          INFINITY    -1855.600000                              100   100
  3:          INFINITY        0.000000                              100   100
    RET       S0

  4:          INFINITY      580.300000                              100   100
    XDE:      0.000000   YDE:  0.000000   ZDE:      0.000000
    XDC:       100       YDC:   100       ZDC:       100
    ADE:    -7.432380    BDE:  0.000000   CDE:      0.000000
    ADC:       100       BDC:   100       CDC:       100

  5:          INFINITY      753.000000                              100   100
    XDE:      0.000000   YDE:  0.000000   ZDE:      0.000000
    XDC:       100       YDC:   100       ZDC:       100
    ADE:   -90.000000    BDE:  0.000000   CDE:      0.000000
    ADC:       100       BDC:   100       CDC:       100

  6:          INFINITY        0.000000                              100   100
    SLB: "front"
  7:          INFINITY     4769.400000                              100   100
  8:          INFINITY        0.000000                              100   100
    SLB: "end"
  9:          INFINITY      287.800000                              100   100
    RET       S6

 10:          INFINITY        0.000000                              100   100
    XDE:      0.000000   YDE:239.600000   ZDE:      0.000000
    XDC:       100       YDC:   100       ZDC:       100
    ADE:      0.000000    BDE:  0.000000   CDE:      0.000000
    ADC:       100       BDC:   100       CDC:       100

 11:          INFINITY        0.000000                              100   100
    XDE:      0.000000   YDE:  0.000000   ZDE:      0.000000
    XDC:       100       YDC:   100       ZDC:       100
    ADE:   -90.000000    BDE:  0.000000   CDE:      0.000000
    ADC:       100       BDC:   100       CDC:       100

 12:          INFINITY        0.000000  REFL                        100   100
    SLB: "mirror1"
 13:          INFINITY      704.700000                              100   100
    RET       S6

 14:          INFINITY        0.000000                              100   100
    XDE:      0.000000   YDE: -88.700000   ZDE:      0.000000
```

```
    XDC:        100          YDC:        100          ZDC:        100
    ADE:      0.000000       BDE:      0.000000       CDE:      0.000000
    ADC:        100          BDC:        100          CDC:        100

15:             INFINITY              0.000000                              100      100
    XDE:      0.000000       YDE:      0.000000       ZDE:      0.000000
    XDC:        100          YDC:        100          ZDC:        100
    ADE:    -38.226767       BDE:    -13.283317       CDE:      0.000000
    ADC:        100          BDC:        100          CDC:        100

16:             INFINITY              0.000000                              100      100
    SLB: "M2dev"
    XDE:      0.000000       YDE:      0.000000       ZDE:      0.000000
    XDC:        100          YDC:        100          ZDC:        100
    ADE:      0.000000       BDE:      0.000000       CDE:      0.000000
    ADC:        100          BDC:        100          CDC:        100

17:          1855.60000             0.000000    REFL                        100      100
    SLB: "mirror2"
    XTO:
    RDX:    3261.30568       CCX:        100
    K    :      0.000000     KC :        100          IC :        YES
    A    :0.000000E+00       B    :0.000000E+00       C    :0.000000E+00       D    :0.000000E+00
    AC :        100          BC :        100          CC :        100          DC :        100
    XDE:      0.000000       YDE:      0.000000       ZDE:      0.000000
    XDC:        100          YDC:        100          ZDC:        100
    ADE:    180.000000       BDE:      0.000000       CDE:     50.754088
    ADC:        100          BDC:        100          CDC:        100

18:             INFINITY            390.500000                              100      100
    RET         S6

19:             INFINITY              0.000000                              100      100
    XDE: -200.000000       YDE:    158.800000       ZDE:      0.000000
    XDC:        100          YDC:        100          ZDC:        100
    ADE:      0.000000       BDE:      0.000000       CDE:      0.000000
    ADC:        100          BDC:        100          CDC:        100

20:             INFINITY              0.000000                              100      100
    XDE:      0.000000       YDE:      0.000000       ZDE:      0.000000
    XDC:        100          YDC:        100          ZDC:        100
    ADE:    -19.865095       BDE:    -13.891460       CDE:      0.000000
    ADC:        100          BDC:        100          CDC:        100

21:             INFINITY              0.000000                              100      100
    SLB: "M3dev"
    XDE:      0.000000       YDE:      0.000000       ZDE:      0.000000
    XDC:        100          YDC:        100          ZDC:        100
    ADE:      0.000000       BDE:      0.000000       CDE:      0.000000
    ADC:        100          BDC:        100          CDC:        100

22:             INFINITY              0.000000    REFL                        100      100
    SLB: "mirror3"
    XTO:
```

```
    RDX: -3295.75965    CCX:        100
    K   :    0.000000   KC :       100          IC :       YES
    A   :0.000000E+00   B  :0.000000E+00   C  :0.000000E+00   D  :0.000000E+00
    AC :       100      BC :       100       CC :       100    DC :       100
    XDE:     0.000000   YDE:     0.000000    ZDE:     0.000000
    XDC:       100      YDC:       100       ZDC:       100
    ADE:   180.000000   BDE:     0.000000    CDE:    46.472120
    ADC:       100      BDC:       100       CDC:       100

23:            INFINITY          0.000000                          100    100
    RET        S6

24:            INFINITY          0.000000                          100    100
    XDE: -200.000000    YDE:   182.700000    ZDE:     0.000000
    XDC:       100      YDC:       100       ZDC:       100
    ADE:     0.000000   BDE:     0.000000    CDE:     0.000000
    ADC:       100      BDC:       100       CDC:       100

25:            INFINITY       1770.000000                          100    100
    XDE:     0.000000   YDE:     0.000000    ZDE:     0.000000
    XDC:       100      YDC:       100       ZDC:       100
    ADE:    -3.500000   BDE:     0.000000    CDE:     0.000000
    ADC:       100      BDC:       100       CDC:       100

26:            INFINITY          0.000000                          100    100
    SLB: "slit"
    XDE:     0.000000   YDE:     0.000000    ZDE:     0.000000   DAR
    XDC:       100      YDC:       100       ZDC:       100
    ADE:    54.572100   BDE:     0.000000    CDE:     0.000000
    ADC:       100      BDC:       100       CDC:       100

27:            INFINITY        330.000000                          100    100
28:         1100.00000         50.000000    SIO2_SCHOTT            100    100
    SLB: "FL1-s1"
29:        -1100.00000          0.000000                          100    100
    SLB: "FL1-s2"
30:            INFINITY       2480.000000                          100    100
    RET        S27

31:          661.52127         35.000000    SIO2_SCHOTT            100    100
    SLB: "RL1-s1"
32:         -768.50404          2.000000                          100    100
    SLB: "RL1-s2"
33:          411.64634         25.000000    SIO2_SCHOTT            100    100
    SLB: "RL2-s1"
34:         1071.79724          0.000000                          100    100
    SLB: "RL2-s2"
35:            INFINITY       2542.000000                          100    100
    RET        S27

36:            INFINITY          0.000000                          100    100
37:            INFINITY          0.000000                          100    100
    RET        S8
```

```
    38:          INFINITY        30.000000         SIO2_SCHOTT          100    100
       SLB: "window-s1"
       XDE: -200.000000    YDE: -105.000000    ZDE:       0.000000
       XDC:        100     YDC:        100     ZDC:        100
       ADE:      0.000000  BDE:      0.000000  CDE:      0.000000
       ADC:        100     BDC:        100     CDC:        100

    39:          INFINITY         0.000000                           100    100
       SLB: "window-s2"
>   40:          INFINITY       659.000000                           100    100
       RET       S36

    41:        -184.48192        25.000000         SIO2_SCHOTT          100    100
       SLB: "FL2-s1"
    42:        -137.49919       200.000000                           100    100
       SLB: "FL2-s2"
    43:       -2651.31077        30.000000         SIO2_SCHOTT          100    100
       SLB: "FOL1-s1f"
       XDE:   -40.000000    YDE:      0.000000    ZDE:      0.000000
       XDC:        100     YDC:        100     ZDC:        100
       ADE:      0.000000  BDE:      0.000000  CDE:      0.000000
       ADC:        100     BDC:        100     CDC:        100

    44:        -420.15415       850.000000                           100    100
       SLB: "FOL1-s2f"
    45:        -340.96322        65.000000         SIO2_SCHOTT          100    100
       SLB: "FOM-s1f"
       XDE:      4.000000    YDE:      6.200000    ZDE:      0.000000
       XDC:        100     YDC:        100     ZDC:        100
       ADE:      0.000000  BDE:      0.000000  CDE:      0.000000
       ADC:        100     BDC:        100     CDC:        100

    46:        -751.65764       -65.000000    REFL SIO2_SCHOTT          100    100
       SLB: "FOM-s2"
    47:        -340.96322      -850.000000                           100    100
       SLB: "FOM-s1s"
    48:        -420.15415       -30.000000         SIO2_SCHOTT          100    100
       SLB: "FOL1-s2s"
       RET       S44

    49:       -2651.31077      -189.963856                           100    100
       SLB: "FOL1-s1s"
    50:          INFINITY         0.000000                           100    100
       XDE:   -32.966000    YDE:      0.000000    ZDE:      0.000000
       XDC:        100     YDC:        100     ZDC:        100
       ADE:      0.000000  BDE:      0.000000  CDE:      0.000000
       ADC:        100     BDC:        100     CDC:        100

    51:          INFINITY       150.000000    REFL                     100    100
       SLB: "mirror4"
       XDE:      0.000000    YDE:      0.000000    ZDE:      0.000000    BEN
       XDC:        100     YDC:        100     ZDC:        100
       ADE:      0.000000  BDE:     45.000000  CDE:      0.000000
       ADC:        100     BDC:        100     CDC:        100
```

```
IMG:        -917.78691        -38.350672                              100     100
    CYL:
    RDX:     INFINITY    CCX:       100
    XDE:     0.000000    YDE:     0.000000    ZDE:     0.000000    DAR
    XDC:       100       YDC:       100       ZDC:       100
    ADE:    25.623547    BDE:     0.000000    CDE:     0.000000
    ADC:       100       BDC:       100       CDC:       100


SPECIFICATION DATA
    EPD         200.00000
    DIM               MM
    WL          1100.00     1000.00      900.00      800.00      700.00      600.00      500.00
                 400.00
    REF               6
    WTW               1           1           1           1           1           1           1
                      1
    XOB         0.00000      0.00000      0.00000      0.00000      0.00000
    YOB       389.00000    194.50000      0.00000   -143.00000   -286.00000
    WTF         1.00000      1.00000      1.00000      1.00000      1.00000
    VUX        -0.95329     -0.95329     -0.95329     -0.95329     -0.95329
    VLX        -0.95329     -0.95329     -0.95329     -0.95329     -0.95329
    VUY        -3.12906     -2.81402     -2.49897     -2.26734     -2.03571
    VLY        -3.95003     -3.57234     -3.19466     -2.91698     -2.63929
    POL               N

APERTURE DATA/EDGE DEFINITIONS
    CA
    CIR S2                  100.000000
    REX S12                  85.000000
    REY S12                 215.000000
    CIR S17                 110.000000
    REX S22                 150.000000
    REY S22                 112.500000
    ADY S22                   2.500000
    CIR S28                 217.000000
    CIR S29                 217.000000
    CIR S31                 150.000000
    CIR S32                 150.000000
    CIR S33                 150.000000
    CIR S34                 150.000000
    CIR S38                  65.000000
    CIR S39                  65.000000
    CIR S41                  90.000000
    CIR S42                  90.000000
    CIR S43                 150.000000
    CIR S44                 150.000000
    CIR S45                 240.000000
    CIR S46                 250.000000
    CIR S47                 240.000000
    CIR S48                 150.000000
    CIR S49                 150.000000
    REX S51                  52.500000
```

REY S51 80.000000

REFRACTIVE INDICES

| GLASS CODE | 1100.00 | 1000.00 | 900.00 | 800.00 | 700.00 | 600.00 | 500.00 | 400.00 |
|---|---|---|---|---|---|---|---|---|
| SIO2_SCHOTT | 1.449177 | 1.450390 | 1.451725 | 1.453288 | 1.455263 | 1.458009 | 1.462299 | 1.470094 |

No solves defined in system

No pickups defined in system

This is a non-symmetric system. If elements with power are decentered or tilted, the first order properties are probably inadequate in describing the system characteristics.

INFINITE CONJUGATES
EFL -849.6799
BFL -568.8357
FFL -871.9292
FNO 4.2484
AT USED CONJUGATES
RED -0.9745
FNO -9.0544
OBJ DIS 0.0000
TT 8916.1183
IMG DIS 111.6493
OAL 8804.4690
PARAXIAL IMAGE
HT 278.7020
THI 259.1626
ANG 54.0092
ENTRANCE PUPIL
DIA 200.0000
THI 1855.6000
EXIT PUPIL
DIA 62.3040
THI -304.1435

## Appendix B Tables of the optical eccentric displacement

Table B-1 The optical eccentric displacement for the view point of F1 with the displacement of the field lens 1 of $\Delta x$=1 mm.

| | | X | Y | Z | TANX | TANY | LENGTH |
|---|---|---|---|---|---|---|---|
| | OBJ | 0 | 0 | 0 | 0 | 0 | 0 |
| | STO | 0 | 0 | 0 | 0 | 0 | 0 |
| front | 6 | 0 | 0 | 0 | 0 | 0 | 0 |
| end | 8 | 0 | 0 | 0 | 0 | 0 | 0 |
| mirror1 | 12 | 0 | 0 | 0 | 0 | 0 | 0 |
| mirror2 | 17 | 0 | 0 | 0 | 0 | 0 | 0 |
| mirror3 | 22 | 0 | 0 | 0 | 0 | 0 | 0 |
| slit | 24 | 0 | 0 | 0 | 0 | 0 | 0 |
| | 25 | 0 | 0 | 0 | 0 | 0 | 0 |
| | 26 | 0 | 0 | 0 | 0 | 0 | 0 |
| | 27 | 0 | 0 | 0 | 0 | 0 | 0 |
| | 28 | 0 | 0 | 0 | 0 | 0 | 0 |
| FL1-s1 | 29 | -1 | 0.00021 | 0.00279 | 0.00029 | 0 | 0.0028 |
| FL1-s2 | 30 | -0.99303 | 0.00019 | -0.00272 | 0.00085 | 0 | -0.0055 |
| | 31 | -0.02433 | 5E-05 | 0 | 0.00085 | 0 | 0.00258 |
| RL-s1 | 32 | 1.7967 | -0.0055 | 0.04571 | -0.00141 | 0 | 0.05435 |
| RL-s2 | 33 | 1.72805 | -0.0021 | 0 | -0.00206 | 0 | -0.04551 |
| | 34 | 1.72805 | -0.0021 | 0 | -0.00206 | 0 | 0 |
| window-s1 | 35 | 0.73997 | -0.00168 | 0 | -0.00141 | 0 | 0.0071 |
| window-s2 | 36 | 0.69759 | -0.00164 | 0 | -0.00207 | 0 | 0.0002 |
| | 37 | 1.74773 | -0.00209 | 0 | -0.00206 | 0 | -0.00754 |
| FL2-s1 | 38 | 0.14288 | -0.00138 | 0 | -0.00141 | 0 | 0.01137 |
| FL2-s2 | 39 | 0.12389 | -0.00129 | -0.00088 | -0.00223 | 1E-05 | -0.00079 |
| FOL-s1f | 40 | -0.12049 | -0.00051 | -0.00533 | -0.00149 | 0 | -0.00218 |
| FOL-s2f | 41 | -0.15809 | -0.00017 | 0.01767 | -0.00206 | 4E-05 | 0.02377 |
| FOM-s1f | 42 | -1.40135 | 0.01625 | -0.04136 | -0.00417 | 6E-05 | 0.04425 |
| FOM-s2s | 43 | -1.57134 | 0.01901 | -0.02882 | -0.00361 | 5E-05 | 0.02376 |
| FOM-s1s | 44 | -1.42731 | 0.02164 | -0.07602 | -0.00117 | 3E-05 | 0.04314 |
| FOL-s2s | 45 | -0.7211 | 0.00492 | -0.07186 | -0.00131 | 2E-05 | -0.05275 |
| FOL-s1s | 46 | -0.68513 | 0.001 | 0.02696 | -0.00218 | 2E-05 | -0.09938 |
| mirror4 | 47 | -0.51554 | 0.00711 | 0 | 0.00439 | -0.00012 | 0.39081 |
| | 48 | -0.2349 | -0.00467 | 0 | 0.00248 | -4E-05 | -0.36268 |
| | IMG | -0.22479 | -0.00454 | -0.00051 | 0.00248 | -4E-05 | -0.00053 |

Table B-2 The optical eccentric displacement for the view point of F1 with the displacement of the field lens 1 of $\Delta y$=1 mm.

| | | X | Y | Z | TANX | TANY | LENGTH |
|---|---|---|---|---|---|---|---|
| | OBJ | 0 | 0 | 0 | 0 | 0 | 0 |
| | STO | 0 | 0 | 0 | 0 | 0 | 0 |
| front | 6 | 0 | 0 | 0 | 0 | 0 | 0 |
| end | 8 | 0 | 0 | 0 | 0 | 0 | 0 |
| mirror1 | 12 | 0 | 0 | 0 | 0 | 0 | 0 |
| mirror2 | 17 | 0 | 0 | 0 | 0 | 0 | 0 |
| mirror3 | 22 | 0 | 0 | 0 | 0 | 0 | 0 |
| slit | 24 | 0 | 0 | 0 | 0 | 0 | 0 |
| | 25 | 0 | 0 | 0 | 0 | 0 | 0 |
| | 26 | 0 | 0 | 0 | 0 | 0 | 0 |
| | 27 | 0 | 0 | 0 | 0 | 0 | 0 |
| | 28 | 0 | 0 | 0 | 0 | 0 | 0 |
| FL1-s1 | 29 | -0.00033 | -1.01165 | -0.15638 | 0 | 0.0003 | -0.15681 |
| FL1-s2 | 30 | 0.00034 | -1.00372 | 0.1552 | 0 | 0.00089 | 0.31159 |
| | 31 | -0.00028 | -0.02612 | 0 | 0 | 0.00089 | -0.15332 |
| RL-s1 | 32 | -0.00112 | 1.87751 | 0.16037 | 0 | -0.00148 | 0.03032 |
| RL-s2 | 33 | -0.00046 | 1.81706 | 0 | -1E-05 | -0.00218 | -0.1555 |
| | 34 | -0.00046 | 1.81706 | 0 | -1E-05 | -0.00218 | 0 |
| window-s1 | 35 | -0.00062 | 0.77905 | 0 | 0 | -0.00148 | 0.06404 |
| window-s2 | 36 | -0.00064 | 0.73455 | 0 | 0 | -0.00222 | 0.00511 |
| | 37 | -0.00042 | 1.83853 | 0 | -1E-05 | -0.00218 | -0.07381 |
| FL2-s1 | 38 | -0.00117 | 0.14184 | 0 | 0 | -0.00148 | 0.18172 |
| FL2-s2 | 39 | -0.00128 | 0.12003 | 0.02508 | 0 | -0.00235 | 0.02662 |
| FOL-s1f | 40 | -0.00082 | -0.13743 | 0.00774 | 0 | -0.00158 | -0.0142 |
| FOL-s2f | 41 | -0.00014 | -0.17672 | -0.02529 | 3E-05 | -0.00216 | -0.03339 |
| FOM-s1f | 42 | 0.02846 | -1.49565 | -0.15697 | 7E-05 | -0.00444 | -0.23882 |
| FOM-s2s | 43 | 0.02531 | -1.67404 | -0.06607 | 8E-05 | -0.00387 | 0.08704 |
| FOM-s1s | 44 | 0.02082 | -1.51365 | -0.1117 | 4E-05 | -0.00128 | 0.06166 |
| FOL-s2s | 45 | 0.01062 | -0.7643 | 0.10154 | 3E-05 | -0.00141 | -0.12625 |
| FOL-s1s | 46 | 0.00774 | -0.72188 | -0.03834 | 5E-05 | -0.00235 | 0.14133 |
| mirror4 | 47 | 0.00089 | -0.37788 | 0 | -1E-04 | 0.00333 | -0.02951 |
| | 48 | -0.00275 | -0.27128 | 0 | -5E-05 | 0.00303 | 0.13989 |
| | IMG | -0.00285 | -0.2443 | -0.02717 | -5E-05 | 0.00303 | -0.03673 |

Table B-3 The optical eccentric displacement for the view point of F1 with the displacement of the field lens 1 of $\Delta z$=1 mm.

| | | X | Y | Z | TANX | TANY | LENGTH |
|---|---|---|---|---|---|---|---|
| | OBJ | 0 | 0 | 0 | 0 | 0 | 0 |
| | STO | 0 | 0 | 0 | 0 | 0 | 0 |
| front | 6 | 0 | 0 | 0 | 0 | 0 | 0 |
| end | 8 | 0 | 0 | 0 | 0 | 0 | 0 |
| mirror1 | 12 | 0 | 0 | 0 | 0 | 0 | 0 |
| mirror2 | 17 | 0 | 0 | 0 | 0 | 0 | 0 |
| mirror3 | 22 | 0 | 0 | 0 | 0 | 0 | 0 |
| slit | 24 | 0 | 0 | 0 | 0 | 0 | 0 |
| | 25 | 0 | 0 | 0 | 0 | 0 | 0 |
| | 26 | 0 | 0 | 0 | 0 | 0 | 0 |
| | 27 | 0 | 0 | 0 | 0 | 0 | 0 |
| | 28 | 0 | 0 | 0 | 0 | 0 | 0 |
| FL1-s1 | 29 | 0.00211 | 0.07536 | 0.01168 | 0 | -2E-05 | 1.01449 |
| FL1-s2 | 30 | 0.00204 | 0.07477 | -0.01159 | 0 | -7E-05 | -0.02328 |
| | 31 | -0.00203 | 0.14522 | 0 | 0 | -7E-05 | -0.99092 |
| RL-s1 | 32 | -0.00571 | 0.00252 | 8E-05 | 0 | -5E-05 | 0.00985 |
| RL-s2 | 33 | -0.00546 | 0.00017 | 0 | 0 | -7E-05 | 9E-05 |
| | 34 | -0.00546 | 0.00017 | 0 | 0 | -7E-05 | 0 |
| window-s1 | 35 | -0.00189 | -0.03426 | 0 | 1E-05 | -5E-05 | 0.0057 |
| window-s2 | 36 | -0.00174 | -0.03572 | 0 | 1E-05 | -8E-05 | 0.00016 |
| | 37 | -0.00552 | 0.00087 | 0 | 0 | -7E-05 | -0.00602 |
| FL2-s1 | 38 | 0.00029 | -0.05459 | 0 | 0 | -5E-05 | 0.00584 |
| FL2-s2 | 39 | 0.00041 | -0.0544 | -0.01139 | 1E-05 | 2E-05 | -0.01137 |
| FOL-s1f | 40 | 0.00103 | -0.05293 | 0.00304 | 1E-05 | 2E-05 | 0.0144 |
| FOL-s2f | 41 | 0.00135 | -0.05242 | -0.00765 | 0 | 9E-05 | -0.01068 |
| FOM-s1f | 42 | 0.0023 | 0.0054 | 0.00061 | 1E-05 | 8E-05 | 0.01282 |
| FOM-s2s | 43 | 0.00258 | 0.0084 | 0.00036 | 1E-05 | -4E-05 | -0.00019 |
| FOM-s1s | 44 | 0.00234 | 0.00969 | 0.0008 | 0 | -8E-05 | -0.0003 |
| FOL-s2s | 45 | -1E-05 | 0.057 | -0.00755 | 0 | -1E-05 | 0.01373 |
| FOL-s1s | 46 | 0.00013 | 0.05688 | 0.00302 | 0 | 1E-05 | -0.01056 |
| mirror4 | 47 | 1E-05 | 0.05556 | 0 | 0 | -1E-05 | 0.00297 |
| | 48 | 6E-05 | 0.06252 | 0 | 0 | -1E-05 | -0.03123 |
| | IMG | 3E-05 | 0.05893 | 0.00657 | 0 | -1E-05 | 0.00749 |

Table B-4 The optical eccentric displacement for the view point of F1 with the displacement of the field lens 1 of $\Delta\alpha$=0.1° .

| | | X | Y | Z | TANX | TANY | LENGTH |
|---|---|---|---|---|---|---|---|
| | OBJ | 0 | 0 | 0 | 0 | 0 | 0 |
| | STO | 0 | 0 | 0 | 0 | 0 | 0 |
| front | 6 | 0 | 0 | 0 | 0 | 0 | 0 |
| end | 8 | 0 | 0 | 0 | 0 | 0 | 0 |
| mirror1 | 12 | 0 | 0 | 0 | 0 | 0 | 0 |
| mirror2 | 17 | 0 | 0 | 0 | 0 | 0 | 0 |
| mirror3 | 22 | 0 | 0 | 0 | 0 | 0 | 0 |
| slit | 24 | 0 | 0 | 0 | 0 | 0 | 0 |
| | 25 | 0 | 0 | 0 | 0 | 0 | 0 |
| | 26 | 0 | 0 | 0 | 0 | 0 | 0 |
| | 27 | 0 | 0 | 0 | 0 | 0 | 0 |
| | 28 | 0 | 0 | 0 | 0 | 0 | 0 |
| FL1-s1 | 29 | -0.00063 | -0.04483 | -0.00695 | 0 | -0.00117 | -0.30189 |
| FL1-s2 | 30 | -0.00059 | -0.07284 | 0.0113 | 1E-05 | -0.0017 | 0.0182 |
| | 31 | 0.00058 | -0.02988 | 0 | 1E-05 | 5E-05 | 0.28368 |
| RL-s1 | 32 | 0.0016 | 0.08332 | 0.00689 | 0 | -6E-05 | -0.00088 |
| RL-s2 | 33 | 0.00156 | 0.08106 | 0 | -1E-05 | -8E-05 | -0.00671 |
| | 34 | 0.00156 | 0.08106 | 0 | -1E-05 | -8E-05 | 0 |
| window-s1 | 35 | 0.00052 | 0.04155 | 0 | 0 | -6E-05 | 0.00168 |
| window-s2 | 36 | 0.00047 | 0.03985 | 0 | 0 | -9E-05 | 0.00019 |
| | 37 | 0.00159 | 0.08188 | 0 | -1E-05 | -8E-05 | -0.00205 |
| FL2-s1 | 38 | -0.00013 | 0.01714 | 0 | 0 | -6E-05 | 0.00687 |
| FL2-s2 | 39 | -0.00017 | 0.01614 | 0.00337 | 0 | -0.00011 | 0.00344 |
| FOL-s1f | 40 | -0.00034 | 0.00435 | -0.00026 | 0 | -8E-05 | -0.0035 |
| FOL-s2f | 41 | -0.00038 | 0.0025 | 0.0004 | 0 | -0.00011 | 0.00064 |
| FOM-s1f | 42 | 0.0004 | -0.06785 | -0.00684 | 0 | -0.00021 | -0.01297 |
| FOM-s2s | 43 | 0.00016 | -0.0764 | -0.00288 | 0 | -0.00017 | 0.00376 |
| FOM-s1s | 44 | 6E-05 | -0.06951 | -0.00486 | 0 | -4E-05 | 0.00265 |
| FOL-s2s | 45 | 0.00033 | -0.04536 | 0.00603 | 0 | -6E-05 | -0.00811 |
| FOL-s1s | 46 | 0.00019 | -0.04346 | -0.00231 | 0 | -0.00011 | 0.00841 |
| mirror4 | 47 | 0 | -0.02784 | 0 | 0 | 0.00016 | -0.00189 |
| | 48 | -0.00013 | -0.02447 | 0 | 0 | 0.00014 | 0.01238 |
| | IMG | -0.00012 | -0.02254 | -0.00251 | 0 | 0.00014 | -0.00313 |

Table B-5 The optical eccentric displacement for the view point of F1 with the displacement of the field lens 1 of $\Delta\beta=0.1^\circ$.

| | | X | Y | Z | TANX | TANY | LENGTH |
|---|---|---|---|---|---|---|---|
| | OBJ | 0 | 0 | 0 | 0 | 0 | 0 |
| | STO | 0 | 0 | 0 | 0 | 0 | 0 |
| front | 6 | 0 | 0 | 0 | 0 | 0 | 0 |
| end | 8 | 0 | 0 | 0 | 0 | 0 | 0 |
| mirror1 | 12 | 0 | 0 | 0 | 0 | 0 | 0 |
| mirror2 | 17 | 0 | 0 | 0 | 0 | 0 | 0 |
| mirror3 | 22 | 0 | 0 | 0 | 0 | 0 | 0 |
| slit | 24 | 0 | 0 | 0 | 0 | 0 | 0 |
| | 25 | 0 | 0 | 0 | 0 | 0 | 0 |
| | 26 | 0 | 0 | 0 | 0 | 0 | 0 |
| | 27 | 0 | 0 | 0 | 0 | 0 | 0 |
| | 28 | 0 | 0 | 0 | 0 | 0 | 0 |
| FL1-s1 | 29 | 0.02266 | -0.00033 | -0.00011 | 0.00119 | 0 | -0.00446 |
| FL1-s2 | 30 | 0.05116 | -0.00033 | 0.00017 | 0.00172 | 0 | 0.00034 |
| | 31 | -0.01221 | -0.0006 | 0 | -3E-05 | 0 | 0.00409 |
| RL-s1 | 32 | -0.08114 | -0.00124 | -0.00192 | 7E-05 | 0 | -0.00216 |
| RL-s2 | 33 | -0.07784 | -0.00131 | 0 | 9E-05 | 0 | 0.0019 |
| | 34 | -0.07784 | -0.00131 | 0 | 9E-05 | 0 | 0 |
| window-s1 | 35 | -0.03024 | -0.00039 | 0 | 7E-05 | 0 | -0.00037 |
| window-s2 | 36 | -0.02821 | -0.00035 | 0 | 1E-04 | 0 | -2E-05 |
| | 37 | -0.07878 | -0.00133 | 0 | 9E-05 | 0 | 0.00039 |
| FL2-s1 | 38 | -0.00148 | 0.00017 | 0 | 7E-05 | 0 | -0.00063 |
| FL2-s2 | 39 | -0.00057 | 0.00019 | 4E-05 | 1E-04 | 0 | 4E-05 |
| FOL-s1f | 40 | 0.0103 | 0.00035 | 0.00044 | 7E-05 | 0 | 0.00031 |
| FOL-s2f | 41 | 0.01196 | 0.00036 | -0.00129 | 8E-05 | 0 | -0.00176 |
| FOM-s1f | 42 | 0.06279 | 0.00059 | 0.0017 | 0.00018 | 0 | -0.00111 |
| FOM-s2s | 43 | 0.07018 | 0.00061 | 0.0012 | 0.00017 | 0 | -0.00097 |
| FOM-s1s | 44 | 0.06356 | 0.00037 | 0.00319 | 6E-05 | 0 | -0.0018 |
| FOL-s2s | 45 | 0.02729 | 0.00022 | 0.00264 | 6E-05 | 0 | 0.00294 |
| FOL-s1s | 46 | 0.02565 | 0.00032 | -0.00098 | 1E-04 | 0 | 0.00365 |
| mirror4 | 47 | 0.01597 | -0.00015 | 0 | -0.00019 | 1E-05 | -0.01223 |
| | 48 | 0.00545 | 9E-05 | 0 | -0.00011 | 0 | 0.01126 |
| | IMG | 0.005 | 9E-05 | 1E-05 | -0.00011 | 0 | 1E-05 |

Table B-6 The optical eccentric displacement for the view point of F3 with the displacement of the field lens 1 of $\Delta x$=1 mm.

| | | X | Y | Z | TANX | TANY | LENGTH |
|---|---|---|---|---|---|---|---|
| | OBJ | 0 | 0 | 0 | 0 | 0 | 0 |
| | STO | 0 | 0 | 0 | 0 | 0 | 0 |
| front | 6 | 0 | 0 | 0 | 0 | 0 | 0 |
| end | 8 | 0 | 0 | 0 | 0 | 0 | 0 |
| mirror1 | 12 | 0 | 0 | 0 | 0 | 0 | 0 |
| mirror2 | 17 | 0 | 0 | 0 | 0 | 0 | 0 |
| mirror3 | 22 | 0 | 0 | 0 | 0 | 0 | 0 |
| slit | 24 | 0 | 0 | 0 | 0 | 0 | 0 |
| | 25 | 0 | 0 | 0 | 0 | 0 | 0 |
| | 26 | 0 | 0 | 0 | 0 | 0 | 0 |
| | 27 | 0 | 0 | 0 | 0 | 0 | 0 |
| | 28 | 0 | 0 | 0 | 0 | 0 | 0 |
| FL1-s1 | 29 | -1 | 0 | 0.00046 | 0.00029 | 0 | 0.00046 |
| FL1-s2 | 30 | -0.98572 | 0 | -0.00044 | 0.00083 | 0 | -0.0009 |
| | 31 | -0.02706 | 0 | 0 | 0.00083 | 0 | 0.00043 |
| RL-s1 | 32 | 1.75056 | 0 | 0.00537 | -0.00136 | 0 | 0.00611 |
| RL-s2 | 33 | 1.68245 | 0 | 0 | -0.00198 | 0 | -0.00532 |
| | 34 | 1.68245 | 0 | 0 | -0.00198 | 0 | 0 |
| window-s1 | 35 | 0.73228 | 0 | 0 | -0.00136 | 0 | 0.00094 |
| window-s2 | 36 | 0.69137 | 0 | 0 | -0.00199 | 0 | 3E-05 |
| | 37 | 1.70117 | 0 | 0 | -0.00198 | 0 | -0.001 |
| FL2-s1 | 38 | 0.15171 | 0 | 0 | -0.00136 | 0 | 0.00154 |
| FL2-s2 | 39 | 0.12446 | 0 | -3E-05 | -0.00217 | 0 | -1E-05 |
| FOL-s1f | 40 | -0.09515 | 1E-05 | -0.00418 | -0.00146 | 0 | -0.00392 |
| FOL-s2f | 41 | -0.14107 | -1E-05 | 0.0155 | -0.00201 | 0 | 0.02035 |
| FOM-s1f | 42 | -1.35481 | -0.00019 | 0.00928 | -0.00403 | 0 | 0.08096 |
| FOM-s2s | 43 | -1.51519 | -0.00011 | -0.00291 | -0.00348 | 0 | -0.00463 |
| FOM-s1s | 44 | -1.37696 | 5E-05 | -0.02137 | -0.00115 | 1E-05 | 0.01248 |
| FOL-s2s | 45 | -0.69035 | -0.00028 | -0.06093 | -0.00127 | 0 | -0.00875 |
| FOL-s1s | 46 | -0.64753 | -0.0004 | 0.0231 | -0.0021 | 0 | -0.08488 |
| mirror4 | 47 | -0.49672 | -1E-05 | 0 | 0.00433 | -0.00001 | 0.37037 |
| | 48 | -0.14056 | -0.00048 | 0 | 0.00243 | 0 | -0.35375 |
| | IMG | -0.14055 | -0.00048 | 0 | 0.00243 | 0 | 0 |

Table B-7 The optical eccentric displacement for the view point of F3 with the displacement of the field lens 1 of $\Delta y$=1 mm.

| | | X | Y | Z | TANX | TANY | LENGTH |
|---|---|---|---|---|---|---|---|
| | OBJ | 0 | 0 | 0 | 0 | 0 | 0 |
| | STO | 0 | 0 | 0 | 0 | 0 | 0 |
| front | 6 | 0 | 0 | 0 | 0 | 0 | 0 |
| end | 8 | 0 | 0 | 0 | 0 | 0 | 0 |
| mirror1 | 12 | 0 | 0 | 0 | 0 | 0 | 0 |
| mirror2 | 17 | 0 | 0 | 0 | 0 | 0 | 0 |
| mirror3 | 22 | 0 | 0 | 0 | 0 | 0 | 0 |
| slit | 24 | 0 | 0 | 0 | 0 | 0 | 0 |
| | 25 | 0 | 0 | 0 | 0 | 0 | 0 |
| | 26 | 0 | 0 | 0 | 0 | 0 | 0 |
| | 27 | 0 | 0 | 0 | 0 | 0 | 0 |
| | 28 | 0 | 0 | 0 | 0 | 0 | 0 |
| FL1-s1 | 29 | 0 | -1 | 0.00048 | 0 | 0.00029 | 0.00048 |
| FL1-s2 | 30 | 0 | -0.98572 | -0.00047 | 0 | 0.00082 | -0.00094 |
| | 31 | 0 | -0.02706 | 0 | 0 | 0.00082 | 0.00045 |
| RL-s1 | 32 | 0 | 1.75056 | 0.00544 | 0 | -0.00136 | 0.0062 |
| RL-s2 | 33 | 0 | 1.68245 | 0 | 0 | -0.00198 | -0.00539 |
| | 34 | 0 | 1.68245 | 0 | 0 | -0.00198 | 0 |
| window-s1 | 35 | 0 | 0.73374 | 0 | 0 | -0.00136 | -0.04385 |
| window-s2 | 36 | 0 | 0.69283 | 0 | 0 | -0.002 | 0.00174 |
| | 37 | 0 | 1.70125 | 0 | 0 | -0.00198 | 0.0413 |
| FL2-s1 | 38 | 0 | 0.1518 | 0 | 0 | -0.00136 | 0.00154 |
| FL2-s2 | 39 | 0 | 0.12454 | -0.00027 | 0 | -0.00217 | -0.00025 |
| FOL-s1f | 40 | 0 | -0.09508 | -4E-05 | 0 | -0.00146 | 0.00066 |
| FOL-s2f | 41 | 0 | -0.14073 | 0.00013 | 0 | -0.00199 | 0.00023 |
| FOM-s1f | 42 | 0.00149 | -1.34318 | -0.0261 | 0 | -0.00399 | -0.02319 |
| FOM-s2s | 43 | 0.00095 | -1.50278 | -0.01282 | 0 | -0.00344 | 0.01455 |
| FOM-s1s | 44 | 0.00023 | -1.36519 | -0.02606 | 0 | -0.00112 | 0.01453 |
| FOL-s2s | 45 | 0.0007 | -0.68597 | 0.00264 | 0 | -0.00125 | -0.02553 |
| FOL-s1s | 46 | 0.00056 | -0.64519 | -0.00101 | 1E-05 | -0.00209 | 0.00373 |
| mirror4 | 47 | 0.00014 | -0.34706 | 0 | 0 | 0.00299 | -0.00046 |
| | 48 | -0.00139 | -0.1642 | 0 | 2E-05 | 0.00277 | 0.0825 |
| | IMG | -0.00139 | -0.16381 | -0.00065 | 2E-05 | 0.00277 | -0.00075 |

Table B-8 The optical eccentric displacement for the view point of F3 with the displacement of the field lens 1 of $\Delta z$=1 mm.

| | | X | Y | Z | TANX | TANY | LENGTH |
|---|---|---|---|---|---|---|---|
| | OBJ | 0 | 0 | 0 | 0 | 0 | 0 |
| | STO | 0 | 0 | 0 | 0 | 0 | 0 |
| front | 6 | 0 | 0 | 0 | 0 | 0 | 0 |
| end | 8 | 0 | 0 | 0 | 0 | 0 | 0 |
| mirror1 | 12 | 0 | 0 | 0 | 0 | 0 | 0 |
| mirror2 | 17 | 0 | 0 | 0 | 0 | 0 | 0 |
| mirror3 | 22 | 0 | 0 | 0 | 0 | 0 | 0 |
| slit | 24 | 0 | 0 | 0 | 0 | 0 | 0 |
| | 25 | 0 | 0 | 0 | 0 | 0 | 0 |
| | 26 | 0 | 0 | 0 | 0 | 0 | 0 |
| | 27 | 0 | 0 | 0 | 0 | 0 | 0 |
| | 28 | 0 | 0 | 0 | 0 | 0 | 0 |
| FL1-s1 | 29 | 0 | -1E-05 | 0 | 0 | 0 | 1 |
| FL1-s2 | 30 | 0 | 0 | 0 | 0 | 0 | 0 |
| | 31 | 0 | -2E-05 | 0 | 0 | 0 | -1 |
| RL-s1 | 32 | 0 | -1E-05 | 0 | 0 | 0 | 0 |
| RL-s2 | 33 | 0 | -1E-05 | 0 | 0 | 0 | 0 |
| | 34 | 0 | -1E-05 | 0 | 0 | 0 | 0 |
| window-s1 | 35 | 0 | 0 | 0 | 0 | 0 | 0 |
| window-s2 | 36 | 0 | 0 | 0 | 0 | 0 | 0 |
| | 37 | 0 | -2E-05 | 0 | 0 | 0 | 0 |
| FL2-s1 | 38 | 0 | 1E-05 | 0 | 0 | 0 | 0 |
| FL2-s2 | 39 | 0 | 0 | 0 | 0 | 0 | 0 |
| FOL-s1f | 40 | 0 | 1E-05 | 0 | 0 | 0 | 0 |
| FOL-s2f | 41 | 0 | 1E-05 | 0 | 0 | 0 | 0 |
| FOM-s1f | 42 | 0 | 1E-05 | 0 | 0 | 0 | 0 |
| FOM-s2s | 43 | 0 | 2E-05 | 0 | 0 | 0 | 0 |
| FOM-s1s | 44 | 0 | 1E-05 | 0 | 0 | 0 | 0 |
| FOL-s2s | 45 | 0 | -1E-05 | 0 | 0 | 0 | 0 |
| FOL-s1s | 46 | 0 | 0 | 0 | 0 | 0 | 0 |
| mirror4 | 47 | 0 | -1E-05 | 0 | 0 | 0 | 0 |
| | 48 | 0 | -1E-05 | 0 | 0 | 0 | 0 |
| | IMG | 0 | -1E-05 | 0 | 0 | 0 | 0 |

Table B-9 The optical eccentric displacement for the view point of F3 with the displacement of the field lens 1 of $\Delta\alpha$=0.1° .

| | | X | Y | Z | TANX | TANY | LENGTH |
|---|---|---|---|---|---|---|---|
| | OBJ | 0 | 0 | 0 | 0 | 0 | 0 |
| | STO | 0 | 0 | 0 | 0 | 0 | 0 |
| front | 6 | 0 | 0 | 0 | 0 | 0 | 0 |
| end | 8 | 0 | 0 | 0 | 0 | 0 | 0 |
| mirror1 | 12 | 0 | 0 | 0 | 0 | 0 | 0 |
| mirror2 | 17 | 0 | 0 | 0 | 0 | 0 | 0 |
| mirror3 | 22 | 0 | 0 | 0 | 0 | 0 | 0 |
| slit | 24 | 0 | 0 | 0 | 0 | 0 | 0 |
| | 25 | 0 | 0 | 0 | 0 | 0 | 0 |
| | 26 | 0 | 0 | 0 | 0 | 0 | 0 |
| | 27 | 0 | 0 | 0 | 0 | 0 | 0 |
| | 28 | 0 | 0 | 0 | 0 | 0 | 0 |
| FL1-s1 | 29 | 0 | 0 | 0 | 0 | -0.00119 | 0.00005 |
| FL1-s2 | 30 | 0 | -0.05985 | 0 | 0 | -0.00172 | 3E-05 |
| | 31 | 0 | 0.02617 | 0 | 0 | 0.00002 | -7E-05 |
| RL-s1 | 32 | 0 | 0.07975 | 0.00001 | 0 | -0.00007 | 2E-05 |
| RL-s2 | 33 | 0 | 0.07621 | 0 | 0 | -0.0001 | -1E-05 |
| | 34 | 0 | 0.07621 | 0 | 0 | -0.0001 | 0 |
| window-s1 | 35 | 0 | 0.02688 | 0 | 0 | -7E-05 | -0.00163 |
| window-s2 | 36 | 0 | 0.02475 | 0 | 0 | -0.0001 | 9E-05 |
| | 37 | 0 | 0.07718 | 0 | 0 | -0.0001 | 0.00151 |
| FL2-s1 | 38 | 0 | -0.00334 | 0 | 0 | -0.00007 | 0 |
| FL2-s2 | 39 | 0 | -0.00476 | 1E-05 | 0 | -0.00009 | 1E-05 |
| FOL-s1f | 40 | 0 | -0.01447 | 0 | 0 | -0.00006 | 0 |
| FOL-s2f | 41 | 0 | -0.01641 | 2E-05 | 0 | -0.00007 | 2E-05 |
| FOM-s1f | 42 | 6E-05 | -0.06084 | -0.00094 | 0 | -0.00017 | -0.00089 |
| FOM-s2s | 43 | 4E-05 | -0.0676 | -0.00046 | 0 | -0.00017 | 0.00053 |
| FOM-s1s | 44 | 2E-05 | -0.06101 | -0.00092 | 0 | -6E-05 | 0.00052 |
| FOL-s2s | 45 | 3E-05 | -0.02079 | 1E-04 | 0 | -6E-05 | -0.00085 |
| FOL-s1s | 46 | 2E-05 | -0.01883 | -3E-05 | 1E-05 | -0.0001 | 0.00013 |
| mirror4 | 47 | 0 | -0.00519 | 0 | 0 | 0.00013 | -2E-05 |
| | 48 | 3E-05 | 0.00482 | 0 | 0 | 0.00013 | -0.00239 |
| | IMG | 3E-05 | 0.00481 | 2E-05 | 0 | 0.00013 | 2E-05 |

Table B-10 The optical eccentric displacement for the view point of F3 with the displacement of the field lens 1 of Δβ=0.1° .

| | | X | Y | Z | TANX | TANY | LENGTH |
|---|---|---|---|---|---|---|---|
| | OBJ | 0 | 0 | 0 | 0 | 0 | 0 |
| | STO | 0 | 0 | 0 | 0 | 0 | 0 |
| front | 6 | 0 | 0 | 0 | 0 | 0 | 0 |
| end | 8 | 0 | 0 | 0 | 0 | 0 | 0 |
| mirror1 | 12 | 0 | 0 | 0 | 0 | 0 | 0 |
| mirror2 | 17 | 0 | 0 | 0 | 0 | 0 | 0 |
| mirror3 | 22 | 0 | 0 | 0 | 0 | 0 | 0 |
| slit | 24 | 0 | 0 | 0 | 0 | 0 | 0 |
| | 25 | 0 | 0 | 0 | 0 | 0 | 0 |
| | 26 | 0 | 0 | 0 | 0 | 0 | 0 |
| | 27 | 0 | 0 | 0 | 0 | 0 | 0 |
| | 28 | 0 | 0 | 0 | 0 | 0 | 0 |
| FL1-s1 | 29 | 0 | 0 | 0 | 0.0012 | 0 | 0 |
| FL1-s2 | 30 | 0.05985 | 0 | 0 | 0.00172 | 0 | 3E-05 |
| | 31 | -0.02617 | 0 | 0 | -0.00002 | 0 | -2E-05 |
| RL-s1 | 32 | -0.07975 | 0 | 0.00001 | 0.00007 | 0 | 1E-05 |
| RL-s2 | 33 | -0.0762 | 0 | 0 | 0.00011 | 0 | -1E-05 |
| | 34 | -0.0762 | 0 | 0 | 0.00011 | 0 | 0 |
| window-s1 | 35 | -0.02683 | 0 | 0 | 0.00007 | 0 | 1E-05 |
| window-s2 | 36 | -0.0247 | 0 | 0 | 0.00011 | 0 | 0 |
| | 37 | -0.07718 | 0 | 0 | 0.00011 | 0 | 0 |
| FL2-s1 | 38 | 0.00334 | 0 | 0 | 0.00007 | 0 | 0 |
| FL2-s2 | 39 | 0.00476 | 0 | 0 | 0.0001 | 0 | 0 |
| FOL-s1f | 40 | 0.01448 | 0 | 0.00064 | 6E-05 | 0 | 0.00064 |
| FOL-s2f | 41 | 0.01645 | 0 | -0.00181 | 8E-05 | 0 | -0.00247 |
| FOM-s1f | 42 | 0.0611 | 0 | -0.00069 | 0.00017 | 0 | -0.00204 |
| FOM-s2s | 43 | 0.06786 | 0 | -1E-05 | 0.00016 | 0 | 0.00038 |
| FOM-s1s | 44 | 0.06127 | -1E-05 | 0.00068 | 6E-05 | 0 | -0.00038 |
| FOL-s2s | 45 | 0.02083 | 0 | 0.00183 | 6E-05 | 0 | 0.00172 |
| FOL-s1s | 46 | 0.01881 | 1E-05 | -0.00066 | 1E-04 | 0 | 0.00253 |
| mirror4 | 47 | 0.00739 | -1E-05 | 0 | -0.00019 | 0 | -0.00569 |
| | 48 | -0.00422 | 0 | 0 | -0.00011 | 0 | 0.00536 |
| | IMG | -0.00422 | 1E-05 | 0 | -0.00011 | 0 | 0 |

Table B-11 The optical eccentric displacement for the view point of F5 with the displacement of the field lens 1 of $\Delta x$=1 mm.

| | | X | Y | Z | TANX | TANY | LENGTH |
|---|---|---|---|---|---|---|---|
| | OBJ | 0 | 0 | 0 | 0 | 0 | 0 |
| | STO | 0 | 0 | 0 | 0 | 0 | 0 |
| front | 6 | 0 | 0 | 0 | 0 | 0 | 0 |
| end | 8 | 0 | 0 | 0 | 0 | 0 | 0 |
| mirror1 | 12 | 0 | 0 | 0 | 0 | 0 | 0 |
| mirror2 | 17 | 0 | 0 | 0 | 0 | 0 | 0 |
| mirror3 | 22 | 0 | 0 | 0 | 0 | 0 | 0 |
| slit | 24 | 0 | 0 | 0 | 0 | 0 | 0 |
| | 25 | 0 | 0 | 0 | 0 | 0 | 0 |
| | 26 | 0 | 0 | 0 | 0 | 0 | 0 |
| | 27 | 0 | 0 | 0 | 0 | 0 | 0 |
| | 28 | 0 | 0 | 0 | 0 | 0 | 0 |
| FL1-s1 | 29 | -1 | 0.00021 | -0.00284 | 0.00029 | 0 | -0.00284 |
| FL1-s2 | 30 | -0.99315 | 0.0002 | 0.00278 | 0.00085 | 0 | 0.00561 |
| | 31 | -0.02429 | 5E-05 | 0 | 0.00085 | 0 | -0.00266 |
| RL-s1 | 32 | 1.79729 | -0.00432 | -0.02985 | -0.0014 | 0 | -0.0372 |
| RL-s2 | 33 | 1.72852 | -0.00204 | 0 | -0.00206 | 0 | 0.02976 |
| | 34 | 1.72852 | -0.00204 | 0 | -0.00206 | 0 | 0 |
| window-s1 | 35 | 0.74857 | -0.00137 | 0 | -0.00141 | 0 | -0.00353 |
| window-s2 | 36 | 0.70646 | -0.00135 | 0 | -0.00204 | 0 | -0.00011 |
| | 37 | 1.7479 | -0.00206 | 0 | -0.00206 | 0 | 0.00376 |
| FL2-s1 | 38 | 0.14347 | -0.00096 | 0 | -0.0014 | 0 | -0.00593 |
| FL2-s2 | 39 | 0.12497 | -0.00089 | 0.0009 | -0.00224 | 0 | 0.00085 |
| FOL-s1f | 40 | -0.1204 | -0.00033 | -0.00522 | -0.0015 | 0 | -0.00767 |
| FOL-s2f | 41 | -0.15759 | -0.00046 | 0.0173 | -0.00205 | -1E-05 | 0.02287 |
| FOM-s1f | 42 | -1.40354 | -0.01247 | 0.04108 | -0.00416 | -4E-05 | 0.1046 |
| FOM-s2s | 43 | -1.57056 | -0.01321 | 0.01276 | -0.00361 | -5E-05 | -0.02242 |
| FOM-s1s | 44 | -1.42641 | -0.01163 | 0.01078 | -0.00119 | -2E-05 | -0.00548 |
| FOL-s2s | 45 | -0.71558 | -0.00517 | -0.05952 | -0.00131 | -2E-05 | 0.01885 |
| FOL-s1s | 46 | -0.6769 | -0.00203 | 0.02249 | -0.00219 | -2E-05 | -0.0829 |
| mirror4 | 47 | -0.52785 | -0.00858 | 0 | 0.00453 | 0.00012 | 0.39047 |
| | 48 | -0.06461 | 0.00491 | 0 | 0.00256 | 3E-05 | -0.38116 |
| | IMG | -0.05348 | 0.00543 | -0.00063 | 0.00256 | 3E-05 | -0.00099 |

Table B-12 The optical eccentric displacement for the view point of F5 with the displacement of the field lens 1 of $\Delta y$=1 mm.

| | | X | Y | Z | TANX | TANY | LENGTH |
|---|---|---|---|---|---|---|---|
| | OBJ | 0 | 0 | 0 | 0 | 0 | 0 |
| | STO | 0 | 0 | 0 | 0 | 0 | 0 |
| front | 6 | 0 | 0 | 0 | 0 | 0 | 0 |
| end | 8 | 0 | 0 | 0 | 0 | 0 | 0 |
| mirror1 | 12 | 0 | 0 | 0 | 0 | 0 | 0 |
| mirror2 | 17 | 0 | 0 | 0 | 0 | 0 | 0 |
| mirror3 | 22 | 0 | 0 | 0 | 0 | 0 | 0 |
| slit | 24 | 0 | 0 | 0 | 0 | 0 | 0 |
| | 25 | 0 | 0 | 0 | 0 | 0 | 0 |
| | 26 | 0 | 0 | 0 | 0 | 0 | 0 |
| | 27 | 0 | 0 | 0 | 0 | 0 | 0 |
| | 28 | 0 | 0 | 0 | 0 | 0 | 0 |
| FL1-s1 | 29 | -0.00022 | -1.01196 | 0.15865 | 0 | 0.0003 | 0.1591 |
| FL1-s2 | 30 | 0.0004 | -1.00426 | -0.15749 | 0 | 0.0009 | -0.31616 |
| | 31 | -0.00025 | -0.02606 | 0 | 0 | 0.0009 | 0.15561 |
| RL-s1 | 32 | -0.00171 | 1.88198 | -0.15236 | 0 | -0.00148 | -0.01972 |
| RL-s2 | 33 | -0.00118 | 1.82054 | 0 | 0 | -0.00218 | 0.14748 |
| | 34 | -0.00118 | 1.82054 | 0 | 0 | -0.00218 | 0 |
| window-s1 | 35 | -0.00121 | 0.77903 | 0 | 0 | -0.00148 | -0.15815 |
| window-s2 | 36 | -0.00119 | 0.73468 | 0 | 1E-05 | -0.00216 | -0.00138 |
| | 37 | -0.00117 | 1.84111 | 0 | 0 | -0.00218 | 0.16234 |
| FL2-s1 | 38 | -0.00087 | 0.14175 | 0 | 0 | -0.00148 | -0.18063 |
| FL2-s2 | 39 | -0.00095 | 0.1204 | -0.02589 | 0 | -0.00236 | -0.02738 |
| FOL-s1f | 40 | -0.00039 | -0.13883 | -0.00803 | 1E-05 | -0.00158 | 0.01561 |
| FOL-s2f | 41 | -0.00058 | -0.17823 | 0.0261 | -2E-05 | -0.00216 | 0.03461 |
| FOM-s1f | 42 | -0.01694 | -1.49841 | 0.10235 | -5E-05 | -0.00444 | 0.18973 |
| FOM-s2s | 43 | -0.01695 | -1.67497 | 0.03928 | -6E-05 | -0.00387 | -0.05643 |
| FOM-s1s | 44 | -0.01379 | -1.51873 | 0.05743 | -3E-05 | -0.00129 | -0.0313 |
| FOL-s2s | 45 | -0.00795 | -0.75376 | -0.09436 | -2E-05 | -0.00141 | 0.07005 |
| FOL-s1s | 46 | -0.0044 | -0.71003 | 0.0356 | -3E-05 | -0.00234 | -0.13134 |
| mirror4 | 47 | -0.00073 | -0.37882 | 0 | 7E-05 | 0.00338 | 0.02805 |
| | 48 | 0.00334 | -0.06407 | 0 | 7E-05 | 0.00321 | 0.0236 |
| | IMG | 0.00349 | -0.05391 | 0.0062 | 7E-05 | 0.00321 | 2E-05 |

Table B-13 The optical eccentric displacement for the view point of F5 with the displacement of the field lens 1 of $\Delta z$=1 mm.

| | | X | Y | Z | TANX | TANY | LENGTH |
|---|---|---|---|---|---|---|---|
| | OBJ | 0 | 0 | 0 | 0 | 0 | 0 |
| | STO | 0 | 0 | 0 | 0 | 0 | 0 |
| front | 6 | 0 | 0 | 0 | 0 | 0 | 0 |
| end | 8 | 0 | 0 | 0 | 0 | 0 | 0 |
| mirror1 | 12 | 0 | 0 | 0 | 0 | 0 | 0 |
| mirror2 | 17 | 0 | 0 | 0 | 0 | 0 | 0 |
| mirror3 | 22 | 0 | 0 | 0 | 0 | 0 | 0 |
| slit | 24 | 0 | 0 | 0 | 0 | 0 | 0 |
| | 25 | 0 | 0 | 0 | 0 | 0 | 0 |
| | 26 | 0 | 0 | 0 | 0 | 0 | 0 |
| | 27 | 0 | 0 | 0 | 0 | 0 | 0 |
| | 28 | 0 | 0 | 0 | 0 | 0 | 0 |
| FL1-s1 | 29 | -0.00136 | -0.07624 | 0.01191 | 0 | 3E-05 | 1.01479 |
| FL1-s2 | 30 | -0.00131 | -0.07565 | -0.01183 | 0 | 7E-05 | -0.02374 |
| | 31 | 0.00294 | -0.14642 | 0 | 0 | 7E-05 | -0.99071 |
| RL-s1 | 32 | 0.00523 | -0.00193 | 6E-05 | 0 | 5E-05 | 0.01001 |
| RL-s2 | 33 | 0.00498 | 0.00043 | 0 | -1E-05 | 7E-05 | 0.00011 |
| | 34 | 0.00498 | 0.00043 | 0 | -1E-05 | 7E-05 | 0 |
| window-s1 | 35 | 0.00148 | 0.03408 | 0 | -0.00001 | 5E-05 | 0.00153 |
| window-s2 | 36 | 0.00132 | 0.03552 | 0 | 0 | 7E-05 | 5E-05 |
| | 37 | 0.00506 | -0.00024 | 0 | -1E-05 | 7E-05 | -0.00166 |
| FL2-s1 | 38 | -0.00067 | 0.05512 | 0 | 0 | 5E-05 | 0.00592 |
| FL2-s2 | 39 | -0.00078 | 0.05488 | -0.01179 | -1E-05 | -2E-05 | -0.01178 |
| FOL-s1f | 40 | -0.00133 | 0.05327 | 0.00302 | 0 | -3E-05 | 0.01479 |
| FOL-s2f | 41 | -0.00134 | 0.05275 | -0.00758 | 0 | -9E-05 | -0.01059 |
| FOM-s1f | 42 | -0.00579 | -0.00618 | 0.00064 | -1E-05 | -8E-05 | 0.01343 |
| FOM-s2s | 43 | -0.00641 | -0.00928 | 0.0003 | -2E-05 | 3E-05 | -0.00021 |
| FOM-s1s | 44 | -0.00575 | -0.01052 | 0.00051 | -1E-05 | 8E-05 | -0.00014 |
| FOL-s2s | 45 | -0.00214 | -0.05764 | -0.0073 | -1E-05 | 1E-05 | 0.01246 |
| FOL-s1s | 46 | -0.0017 | -0.05757 | 0.00292 | -1E-05 | -1E-05 | -0.01021 |
| mirror4 | 47 | -0.00017 | -0.05627 | 0 | 3E-05 | 2E-05 | 0.00297 |
| | 48 | 0.00089 | -0.06431 | 0 | 2E-05 | 1E-05 | 0.03192 |
| | IMG | 0.00077 | -0.0691 | 0.00795 | 2E-05 | 1E-05 | 0.00929 |

Table B-14 The optical eccentric displacement for the view point of F5 with the displacement of the field lens 1 of $\Delta\alpha$=0.1° .

| | | X | Y | Z | TANX | TANY | LENGTH |
|---|---|---|---|---|---|---|---|
| | OBJ | 0 | 0 | 0 | 0 | 0 | 0 |
| | STO | 0 | 0 | 0 | 0 | 0 | 0 |
| front | 6 | 0 | 0 | 0 | 0 | 0 | 0 |
| end | 8 | 0 | 0 | 0 | 0 | 0 | 0 |
| mirror1 | 12 | 0 | 0 | 0 | 0 | 0 | 0 |
| mirror2 | 17 | 0 | 0 | 0 | 0 | 0 | 0 |
| mirror3 | 22 | 0 | 0 | 0 | 0 | 0 | 0 |
| slit | 24 | 0 | 0 | 0 | 0 | 0 | 0 |
| | 25 | 0 | 0 | 0 | 0 | 0 | 0 |
| | 26 | 0 | 0 | 0 | 0 | 0 | 0 |
| | 27 | 0 | 0 | 0 | 0 | 0 | 0 |
| | 28 | 0 | 0 | 0 | 0 | 0 | 0 |
| FL1-s1 | 29 | -0.00041 | -0.0462 | 0.00722 | 0 | -0.00116 | 0.30462 |
| FL1-s2 | 30 | -0.00038 | -0.07364 | -0.01152 | 0 | -0.00169 | -0.01866 |
| | 31 | 0.00085 | -0.03091 | 0 | 0 | 6E-05 | -0.28594 |
| RL-s1 | 32 | 0.00144 | 0.08626 | -0.00728 | 0 | -6E-05 | 0.0008 |
| RL-s2 | 33 | 0.00139 | 0.08395 | 0 | 0 | -9E-05 | 0.0071 |
| | 34 | 0.00139 | 0.08395 | 0 | 0 | -9E-05 | 0 |
| window-s1 | 35 | 0.00037 | 0.04278 | 0 | 0 | -6E-05 | -0.00702 |
| window-s2 | 36 | 0.00032 | 0.04102 | 0 | 0 | -9E-05 | -6E-05 |
| | 37 | 0.00142 | 0.08475 | 0 | 0 | -9E-05 | 0.00719 |
| FL2-s1 | 38 | -0.00025 | 0.01769 | 0 | 0 | -6E-05 | -0.0072 |
| FL2-s2 | 39 | -0.00028 | 0.01665 | -0.00358 | 0 | -0.00011 | -0.00364 |
| FOL-s1f | 40 | -0.00042 | 0.00439 | 0.00023 | 0 | -8E-05 | 0.00369 |
| FOL-s2f | 41 | -0.00045 | 0.00248 | -0.00032 | 0 | -0.00011 | -0.00053 |
| FOM-s1f | 42 | -0.00231 | -0.07024 | 0.00516 | 0 | -0.00022 | 0.01171 |
| FOM-s2s | 43 | -0.00247 | -0.079 | 0.00202 | -1E-05 | -0.00017 | -0.00282 |
| FOM-s1s | 44 | -0.00214 | -0.07204 | 0.00306 | -1E-05 | -4E-05 | -0.00165 |
| FOL-s2s | 45 | -0.00088 | -0.04641 | -0.00581 | 0 | -6E-05 | 0.00601 |
| FOL-s1s | 46 | -0.00062 | -0.04437 | 0.00222 | 0 | -0.00011 | -0.00809 |
| mirror4 | 47 | -5E-05 | -0.02886 | 0 | 1E-05 | 0.00016 | 0.00185 |
| | 48 | 0.00043 | -0.016 | 0 | 1E-05 | 0.00015 | 0.00756 |
| | IMG | 0.00041 | -0.01651 | 0.0019 | 1E-05 | 0.00015 | 0.00189 |

Table B-15 The optical eccentric displacement for the view point of F5 with the displacement of the field lens 1 of Δβ=0.1° .

| | | X | Y | Z | TANX | TANY | LENGTH |
|---|---|---|---|---|---|---|---|
| | OBJ | 0 | 0 | 0 | 0 | 0 | 0 |
| | STO | 0 | 0 | 0 | 0 | 0 | 0 |
| front | 6 | 0 | 0 | 0 | 0 | 0 | 0 |
| end | 8 | 0 | 0 | 0 | 0 | 0 | 0 |
| mirror1 | 12 | 0 | 0 | 0 | 0 | 0 | 0 |
| mirror2 | 17 | 0 | 0 | 0 | 0 | 0 | 0 |
| mirror3 | 22 | 0 | 0 | 0 | 0 | 0 | 0 |
| slit | 24 | 0 | 0 | 0 | 0 | 0 | 0 |
| | 25 | 0 | 0 | 0 | 0 | 0 | 0 |
| | 26 | 0 | 0 | 0 | 0 | 0 | 0 |
| | 27 | 0 | 0 | 0 | 0 | 0 | 0 |
| | 28 | 0 | 0 | 0 | 0 | 0 | 0 |
| FL1-s1 | 29 | 0.02304 | -0.00048 | 0.00015 | 0.00119 | 0 | 0.00638 |
| FL1-s2 | 30 | 0.05104 | -0.00047 | -0.00024 | 0.00171 | 0 | -0.00042 |
| | 31 | -0.01197 | -0.00089 | 0 | -3E-05 | 0 | -0.00592 |
| RL-s1 | 32 | -0.08132 | -0.00052 | 0.00168 | 7E-05 | 0 | 0.00201 |
| RL-s2 | 33 | -0.07801 | -0.0006 | 0 | 0.0001 | 0 | -0.00167 |
| | 34 | -0.07801 | -0.0006 | 0 | 0.0001 | 0 | 0 |
| window-s1 | 35 | -0.03075 | -2E-05 | 0 | 6E-05 | 0 | 0.0003 |
| window-s2 | 36 | -0.02873 | 0 | 0 | 0.0001 | 0 | 1E-05 |
| | 37 | -0.07894 | -0.00061 | 0 | 0.0001 | 0 | -0.00031 |
| FL2-s1 | 38 | -0.00157 | 0.00034 | 0 | 7E-05 | 0 | 0.00048 |
| FL2-s2 | 39 | -0.00068 | 0.00034 | -7E-05 | 0.0001 | 0 | -7E-05 |
| FOL-s1f | 40 | 0.01027 | 0.0004 | 0.00047 | 7E-05 | 0 | 0.00062 |
| FOL-s2f | 41 | 0.01189 | 0.00042 | -0.00137 | 9E-05 | 1E-05 | -0.00185 |
| FOM-s1f | 42 | 0.06305 | 0.00093 | -0.00216 | 0.00018 | 0 | -0.00406 |
| FOM-s2s | 43 | 0.07033 | 0.001 | -0.00073 | 0.00017 | 0 | 0.00119 |
| FOM-s1s | 44 | 0.06368 | 0.00087 | -0.00079 | 6E-05 | 0 | 0.00042 |
| FOL-s2s | 45 | 0.02724 | 8E-05 | 0.00223 | 6E-05 | 0 | -0.00031 |
| FOL-s1s | 46 | 0.02547 | -5E-05 | -0.00083 | 1E-04 | 0 | 0.00311 |
| mirror4 | 47 | 0.01661 | 6E-05 | 0 | -0.0002 | 0 | -0.01233 |
| | 48 | -0.00209 | -0.00051 | 0 | -0.00011 | 0 | 0.01227 |
| | IMG | -0.0026 | -0.00056 | 6E-05 | -0.00011 | 0 | 9E-05 |

# 国際単位系（SI）

表１．SI 基本単位

| 基本量 | SI 基本単位 | |
|---|---|---|
| | 名称 | 記号 |
| 長さ | メートル | m |
| 質量 | キログラム | kg |
| 時間 | 秒 | s |
| 電流 | アンペア | A |
| 熱力学温度 | ケルビン | K |
| 物質量 | モル | mol |
| 光度 | カンデラ | cd |

表２．基本単位を用いて表されるSI組立単位の例

| 組立量 | SI 基本単位 | |
|---|---|---|
| | 名称 | 記号 |
| 面積 | 平方メートル | $m^2$ |
| 体積 | 立法メートル | $m^3$ |
| 速さ，速度 | メートル毎秒 | m/s |
| 加速度 | メートル毎秒毎秒 | $m/s^2$ |
| 波数 | 毎メートル | $m^{-1}$ |
| 密度（質量密度） | キログラム毎立法メートル | $kg/m^3$ |
| 質量体積（比体積） | 立法メートル毎キログラム | $m^3/kg$ |
| 電流密度 | アンペア毎平方メートル | $A/m^2$ |
| 磁界の強さ | アンペア毎メートル | A/m |
| （物質量の）濃度 | モル毎立方メートル | $mol/m^3$ |
| 輝度 | カンデラ毎平方メートル | $cd/m^2$ |
| 屈折率 | （数の）1 | 1 |

表５．SI 接頭語

| 乗数 | 接頭語 | 記号 | 乗数 | 接頭語 | 記号 |
|---|---|---|---|---|---|
| $10^{24}$ | ヨタ | Y | $10^{-1}$ | デシ | d |
| $10^{21}$ | ゼタ | Z | $10^{-2}$ | センチ | c |
| $10^{18}$ | エクサ | E | $10^{-3}$ | ミリ | m |
| $10^{15}$ | ペタ | P | $10^{-6}$ | マイクロ | μ |
| $10^{12}$ | テラ | T | $10^{-9}$ | ナノ | n |
| $10^{9}$ | ギガ | G | $10^{-12}$ | ピコ | p |
| $10^{6}$ | メガ | M | $10^{-15}$ | フェムト | f |
| $10^{3}$ | キロ | k | $10^{-18}$ | アト | a |
| $10^{2}$ | ヘクト | h | $10^{-21}$ | ゼプト | z |
| $10^{1}$ | デカ | da | $10^{-24}$ | ヨクト | y |

表３．固有の名称とその独自の記号で表されるSI組立単位

| 組立量 | SI 組立単位 | | | |
|---|---|---|---|---|
| | 名称 | 記号 | 他のSI単位による表し方 | SI基本単位による表し方 |
| 平面角 | ラジアン(a) | rad | | $m \cdot m^{-1}=1$(b) |
| 立体角 | ステラジアン(a) | sr(c) | | $m^2 \cdot m^{-2}=1$(b) |
| 周波数 | ヘルツ | Hz | | $s^{-1}$ |
| 力 | ニュートン | N | | $m \cdot kg \cdot s^{-2}$ |
| 圧力，応力 | パスカル | Pa | $N/m^2$ | $m^{-1} \cdot kg \cdot s^{-2}$ |
| エネルギー，仕事，熱量 | ジュール | J | N・m | $m^2 \cdot kg \cdot s^{-2}$ |
| 工率，放射束 | ワット | W | J/s | $m^2 \cdot kg \cdot s^{-3}$ |
| 電荷，電気量 | クーロン | C | | s・A |
| 電位差（電圧），起電力 | ボルト | V | W/A | $m^2 \cdot kg \cdot s^{-3} \cdot A^{-1}$ |
| 静電容量 | ファラド | F | C/V | $m^{-2} \cdot kg^{-1} \cdot s^4 \cdot A^2$ |
| 電気抵抗 | オーム | Ω | V/A | $m^2 \cdot kg \cdot s^{-3} \cdot A^{-2}$ |
| コンダクタンス | ジーメンス | S | A/V | $m^{-2} \cdot kg^{-1} \cdot s^3 \cdot A^2$ |
| 磁束 | ウエーバ | Wb | V・s | $m^2 \cdot kg \cdot s^{-2} \cdot A^{-1}$ |
| 磁束密度 | テスラ | T | $Wb/m^2$ | $kg \cdot s^{-2} \cdot A^{-1}$ |
| インダクタンス | ヘンリー | H | Wb/A | $m^2 \cdot kg \cdot s^{-2} \cdot A^{-2}$ |
| セルシウス温度 | セルシウス度(d) | ℃ | | K |
| 光束 | ルーメン | lm | cd・sr(c) | $m^2 \cdot m^{-2} \cdot cd=cd$ |
| 照度 | ルクス | lx | $lm/m^2$ | $m^2 \cdot m^{-4} \cdot cd=m^{-2} \cdot cd$ |
| （放射性核種の）放射能 | ベクレル | Bq | | $s^{-1}$ |
| 吸収線量，質量エネルギー分与，カーマ | グレイ | Gy | J/kg | $m^2 \cdot s^{-2}$ |
| 線量当量，周辺線量当量，方向性線量当量，個人線量当量，組織線量当 | シーベルト | Sv | J/kg | $m^2 \cdot s^{-2}$ |

(a)ラジアン及びステラジアンの使用は、同じ次元であっても異なった性質をもった量を区別するときの組立単位の表し方として利点がある。組立単位を形作るときのいくつかの用例は表４に示されている。
(b)実際には、使用する時には記号rad及びsrが用いられるが、習慣として組立単位としての記号“１”は明示されない。
(c)測光学では、ステラジアンの名称と記号srを単位の表し方の中にそのまま維持している。
(d)この単位は、例としてミリセルシウス度m℃のようにSI接頭語を伴って用いても良い。

表４．単位の中に固有の名称とその独自の記号を含むSI組立単位の例

| 組立量 | SI 組立単位 | | |
|---|---|---|---|
| | 名称 | 記号 | SI 基本単位による表し方 |
| 粘度 | パスカル秒 | Pa・s | $m^{-1} \cdot kg \cdot s^{-1}$ |
| 力のモーメント | ニュートンメートル | N・m | $m^2 \cdot kg \cdot s^{-2}$ |
| 表面張力 | ニュートン毎メートル | N/m | $kg \cdot s^{-2}$ |
| 角速度 | ラジアン毎秒 | rad/s | $m \cdot m^{-1} \cdot s^{-1}=s^{-1}$ |
| 角加速度 | ラジアン毎平方秒 | $rad/s^2$ | $m \cdot m^{-1} \cdot s^{-2}=s^{-2}$ |
| 熱流密度，放射照度 | ワット毎平方メートル | $W/m^2$ | $kg \cdot s^{-3}$ |
| 熱容量，エントロピー | ジュール毎ケルビン | J/K | $m^2 \cdot kg \cdot s^{-2} \cdot K^{-1}$ |
| 質量熱容量（比熱容量），質量エントロピー | ジュール毎キログラム毎ケルビン | J/(kg・K) | $m^2 \cdot s^{-2} \cdot K^{-1}$ |
| 質量エネルギー（比エネルギー） | ジュール毎キログラム | J/kg | $m^2 \cdot s^{-2} \cdot K^{-1}$ |
| 熱伝導率 | ワット毎メートル毎ケルビン | W/(m・K) | $m \cdot kg \cdot s^{-3} \cdot K^{-1}$ |
| 体積エネルギー | ジュール毎立方メートル | $J/m^3$ | $m^{-1} \cdot kg \cdot s^{-2}$ |
| 電界の強さ | ボルト毎メートル | V/m | $m \cdot kg \cdot s^{-3} \cdot A^{-1}$ |
| 体積電荷 | クーロン毎立方メートル | $C/m^3$ | $m^{-3} \cdot s \cdot A$ |
| 電気変位 | クーロン毎平方メートル | $C/m^2$ | $m^{-2} \cdot s \cdot A$ |
| 誘電率 | ファラド毎メートル | F/m | $m^{-3} \cdot kg^{-1} \cdot s^4 \cdot A^2$ |
| 透磁率 | ヘンリー毎メートル | H/m | $m \cdot kg \cdot s^{-2} \cdot A^{-2}$ |
| モルエネルギー | ジュール毎モル | J/mol | $m^2 \cdot kg \cdot s^{-2} \cdot mol^{-1}$ |
| モルエントロピー，モル熱容量 | ジュール毎モル毎ケルビン | J/(mol・K) | $m^2 \cdot kg \cdot s^{-2} \cdot K^{-1} \cdot mol^{-1}$ |
| 照射線量（X線及びγ線） | クーロン毎キログラム | C/kg | $kg^{-1} \cdot s \cdot A$ |
| 吸収線量率 | グレイ毎秒 | Gy/s | $m^2 \cdot s^{-3}$ |
| 放射強度 | ワット毎ステラジアン | W/sr | $m^4 \cdot m^{-2} \cdot kg \cdot s^{-3}=m^2 \cdot kg \cdot s^{-3}$ |
| 放射輝度 | ワット毎平方メートル毎ステラジアン | $W/(m^2 \cdot sr)$ | $m^2 \cdot m^{-2} \cdot kg \cdot s^{-3}=kg \cdot s^{-3}$ |

表６．国際単位系と併用されるが国際単位系に属さない単位

| 名称 | 記号 | SI 単位による値 |
|---|---|---|
| 分 | min | 1 min=60s |
| 時 | h | 1h =60 min=3600 s |
| 日 | d | 1 d=24 h=86400 s |
| 度 | ° | 1°=(π/180) rad |
| 分 | ’ | 1’=(1/60)°=(π/10800) rad |
| 秒 | ” | 1”=(1/60)’=(π/648000) rad |
| リットル | l、L | 1l=1 $dm^3=10^{-3}m^3$ |
| トン | t | 1t=$10^3$ kg |
| ネーパ | Np | 1Np=1 |
| ベル | B | 1B=(1/2)ln10(Np) |

表７．国際単位系と併用されこれに属さない単位でSI単位で表される数値が実験的に得られるもの

| 名称 | 記号 | SI 単位であらわされる数値 |
|---|---|---|
| 電子ボルト | eV | 1eV=1.60217733(49)×$10^{-19}$J |
| 統一原子質量単位 | u | 1u=1.6605402(10)×$10^{-27}$kg |
| 天文単位 | ua | 1ua=1.49597870691(30)×$10^{11}$m |

表８．国際単位系に属さないが国際単位系と併用されるその他の単位

| 名称 | 記号 | SI 単位であらわされる数値 |
|---|---|---|
| 海里 | | 1海里=1852m |
| ノット | | 1ノット=1海里毎時=(1852/3600)m/s |
| アール | a | 1 a=1 $dam^2=10^2m^2$ |
| ヘクタール | ha | 1 ha=1 $hm^2=10^4m^2$ |
| バール | bar | 1 bar=0.1MPa=100kPa=1000hPa=$10^5$Pa |
| オングストローム | Å | 1 Å=0.1nm=$10^{-10}$m |
| バーン | b | 1 b=100$fm^2=10^{-28}m^2$ |

表９．固有の名称を含むCGS組立単位

| 名称 | 記号 | SI 単位であらわされる数値 |
|---|---|---|
| エルグ | erg | 1 erg=$10^{-7}$ J |
| ダイン | dyn | 1 dyn=$10^{-5}$N |
| ポアズ | P | 1 P=1 dyn・s/$cm^2$=0.1Pa・s |
| ストークス | St | 1 St =$1cm^2/s=10^{-4}m^2/s$ |
| ガウス | G | 1 G ^10$^{-4}$T |
| エルステッド | Oe | 1 Oe ^(1000/4π)A/m |
| マクスウェル | Mx | 1 Mx ^10$^{-8}$Wb |
| スチルブ | sb | 1 sb =$1cd/cm^2=10^4cd/m^2$ |
| ホト | ph | 1 ph=$10^4$lx |
| ガル | Gal | 1 Gal =$1cm/s^2=10^{-2}m/s^2$ |

表10．国際単位に属さないその他の単位の例

| 名称 | 記号 | SI 単位であらわされる数値 |
|---|---|---|
| キュリー | Ci | 1 Ci=3.7×$10^{10}$Bq |
| レントゲン | R | 1 R = 2.58×$10^{-4}$C/kg |
| ラド | rad | 1 rad=1cGy=$10^{-2}$Gy |
| レム | rem | 1 rem=1 cSv=$10^{-2}$Sv |
| X線単位 | | 1X unit=1.002×$10^{-4}$nm |
| ガンマ | γ | 1γ=1 nT=$10^{-9}$T |
| ジャンスキー | Jy | 1 Jy=$10^{-26}$W・$m^{-2}$・$Hz^{-1}$ |
| フェルミ | | 1 fermi=1 fm=$10^{-15}$m |
| メートル系カラット | | 1 metric carat = 200 mg = 2×$10^{-4}$kg |
| トル | Torr | 1 Torr = (101 325/760) Pa |
| 標準大気圧 | atm | 1 atm = 101 325 Pa |
| カロリー | cal | |
| ミクロン | μ | 1 μ =1μm=$10^{-6}$m |

（第７版，1998年改訂）